JOURNAL OF CATALYSIS 6, 108–136 (1966)

# Effects of Oxygen Sorption on the Ferromagnetic Properties of Small Nickel Particles

J. W. GEUS AND A. P. P. NOBEL

*From the Central Laboratory, Staatsmijnen in Limburg, Geleen, The Netherlands*

Received December 29, 1965

Measurements on the effects of oxygen sorption on the low-field magnetization of nickel are reported. An investigation was made of three types of nickel-on-inert-support catalysts containing very small or larger (up to 140 Å diameter) nickel particles.

The oxygen sorbed was taken either from nitrous oxide, which decomposes on nickel into oxygen and nitrogen, or from molecular oxygen. It is shown that oxygen is adsorbed homogeneously by the nickel particles interacting with nitrous oxide, and the interaction remains restricted to about the first layer of nickel atoms at room temperature. Admission of molecular oxygen to a nickel catalyst causes the nickel particles to be partially oxidized successively.

From the experimental results it is concluded that the oxygen sorption affects the ferromagnetism of nickel by decoupling the magnetic moments of the chemisorbing metal surface atoms from the moment of the remainder of the metal. In completely superparamagnetic systems this brings about a decrease in magnetization that is larger on adsorption from nitrous oxide than on sorption from molecular oxygen owing to the difference in distribution of the adsorbed atoms.

Measurements with magnetizing fields of different frequencies clearly demonstrate the effect of oxygen sorption on both the ferromagnetic moment and the ferromagnetic anisotropy. It is shown that the distribution of the oxygen atoms sorbed can even determine whether the resulting change in magnetization will be positive or negative, when incompletely superparamagnetic systems are investigated. The effect on the anisotropy can be ascribed to a decrease in the surface area of the ferromagnetic phase caused by the sorption of oxygen. Finally, the implications of a remaining weak coupling of the moments of the chemisorbing nickel atoms to the ferromagnetic core are discussed.

## INTRODUCTION

Only a limited number of investigations into the effects of oxygen sorption on the magnetization of small nickel particles have been performed up to now. The first experiments were done by Moore and Selwood (*1*), who erroneously found an increase in magnetization on sorption of oxygen.

Broeder, van Reijen, and Korswagen (*2*) obtained the first reliable results. In experiments at room temperature they found that, per unit volume of gas uptake, oxygen decreases the magnetization to about the same extent as hydrogen.

These results were confirmed by Leak and Selwood (*3*). These authors, moreover, observed that at −78°C the magnetization at first very slightly increased upon oxygen sorption, whereas on further adsorption it decreased. Adsorption of hydrogen, on the same catalyst and at the same temperature, strongly increased the magnetization. At −78°C the decrease brought about by oxygen sorption was markedly smaller than that observed at room temperature for the same catalyst. When the oxygen was taken from nitrous oxide, which decomposes on nickel into oxygen and nitrogen, the results were completely different. In this case the magnetization strongly increased as it did upon hydrogen adsorption (*4*). Finally, it was found in this laboratory that oxygen decreases the magnetization to the same extent as hydrogen (*5*) only if the system

behaves completely superparamagnetically under the conditions of the experiment. In these experiments the oxygen was taken from molecular oxygen. When the system was not completely superparamagnetic, the effects of hydrogen and oxygen were clearly different.

It was demonstrated that chemisorption on nickel particles has a twofold effect on the ferromagnetic properties, viz. a decrease in the magnetic moment of the nickel particles and a decrease in the ferromagnetic anisotropy energy. This last effect is apparent if measurements are done on not completely superparamagnetic systems. From the experimental evidence mentioned above it might be concluded that the effects of oxygen and hydrogen on the magnetic moment of the nickel particles are the same, whereas the anisotropy energy is affected much less by sorption from molecular oxygen. In view of the different effects on the anisotropy energy in the nitrous oxide and in the molecular oxygen experiments, which are suggested by the results of Leak and Selwood (*3*), more experimental evidence is highly desirable. First, the effect on completely superparamagnetic systems of oxygen sorption from nitrous oxide has to be investigated. Secondly, the effects of sorption from molecular oxygen and from nitrous oxide are to be determined on systems of which the extent of deviation from superparamagnetic behavior is known. In this paper extensive measurements on these points are reported for three different, well-defined catalysts.

## Experimental

**a. Measurement of the magnetization.** The apparatus was the same as that described earlier (*5*) but for the following minor modifications: The coils of the measuring and the reference cell that were wound on asbestos were replaced by a more stable arrangement. By etching with hydrofluoric acid 33 turns were grooved directly into the glass walls of the cells. In these grooves 0.2-mm platinum-iridium wire was wound. The alloy contains 20% Ir; it retains its elasticity up to fairly high temperatures. The coils can be heated for prolonged times above 500°C without any change. The sensitivity was increased by insertion of a 50c/sec filter in the measuring circuit. When catalysts displaying high signals (around 10 mV or more) were measured, the accuracy of the determination of the effects of sorption was increased by replacing the empty reference cell by a cell filled with about the same amount of catalyst as the measuring cell. This catalyst was reduced and evacuated and remained unaltered while the sorption in the measuring cell proceeded.

To obtain all temperatures between 77° and 500°K, a system with streaming nitrogen was used. For temperatures below room temperature the nitrogen was cooled by passing it through a copper coil placed in liquid nitrogen; for temperatures higher than room temperature the nitrogen was passed along an electrically heated wire. The temperature was controlled by varying the nitrogen flow rate. The cooled or heated nitrogen was circulated in the space between the measuring cell and an insulating Dewar vessel which surrounded the cell.

**b. Materials.** The investigations described here were performed with three types of nickel catalysts. One type was prepared by a method recently developed in this laboratory. A very homogeneous distribution of nickel hydroxide over the surface of the support is obtained by precipitation from a homogeneous solution on a supporting material suspended in the solution. In a forthcoming paper full details of this preparation technique and of the properties of the resulting catalysts will be given.

These catalysts, dried at 120°C, are virtually completely reduced by heating them in flowing hydrogen at 370°C for about 70 hr. This was found by determining the weight changes upon heating in hydrogen by means of a thermobalance. Two different samples of this type were investigated which, after being dried at 120°C, contained 35.4% and 40.9% nickel, respectively.

As will be shown below, the homogeneously precipitated catalysts contain rather small nickel particles. To perform measurements on larger nickel particles a commercial nickel-on-silica catalyst was used (Harshaw Ni-0104 P nickel-on-kieselguhr). This cata-

lyst as received is partially reduced; in this condition the nickel content is 58.5%. Some measurements were done on another commercial nickel catalyst (Girdler G-12 nickel-on-alumina). Before reduction this catalyst contains 51% nickel.

For the reduction of the catalysts use was made of tank hydrogen, which was purified by passing it through a "deoxo" catalyst and through a trap cooled at 77°K. Oxygen was obtained by decomposition of well-degassed potassium permanganate, and nitrous oxide was taken from a cylinder. Mass spectrometric analysis gave the following composition: $O_2$, 0.15%; $N_2$, 1.2%; $N_2O$, 98.6%; Ar, 0.01%.

**c. Methods.** The catalysts were reduced and evacuated in the measuring cell. The hydrogen flow rate was about 10 liter/hr. After reduction the catalysts were evacuated for 16 hr at a slightly lower temperature. Evacuation was effected by means of a mercury diffusion pump backed by a rotary oil pump. Measurements were performed only when the pressure was below $10^{-5}$ mm Hg and the catalyst was at the evacuation temperature. To ensure a good thermal contact carefully purified helium was admitted up to a pressure of about 0.7 mm Hg after evacuation, cooling to room temperature, and disconnection from the pumps.

Gases were supplied from a standard gas-metering system. To protect the catalysts against mercury vapor, a cold trap was inserted just before the measuring cell. During the measurement of molecular oxygen sorption this trap was cooled at 77°K, whereas a temperature of only 195°K was used in the experiments with nitrous oxide, which has a relatively high boiling point.

Since the decomposition of nitrous oxide does not give rise to a decrease in pressure, the amount of oxygen sorbed by this decomposition was calculated from the nitrogen enrichment in the gas, which was determined mass-spectrometrically. The nitrous oxide was concentrated on the catalyst by cooling the latter to 77°K; at this temperature all nitrous oxide is physisorbed on the samples. Then the metering system is disconnected from the measuring cell and the catalyst is heated to room temperature. After 16 hr of contact the nitrous oxide had generally decomposed for 95% or more. For shorter contact times the decomposition was accelerated by repeatedly cooling the catalyst to 77°K and heating again to room temperature.

To characterize the catalysts as well as possible the total surface area and the size of the nickel particles were determined separately. The total surface area was calculated from the physical adsorption of nitrogen according to the BET theory; for the surface area of a nitrogen molecule 15.4 Å$^2$ was taken. By various means the size of the nickel particles in the catalysts was determined: X-ray line-broadening, electron microscopic investigation, and measurement of the extent of hydrogen adsorption. The X-ray line-broadening of the reduced and degassed catalysts was determined in a standard way. Before electron micrographs were taken, the catalysts were reduced and evacuated. The evacuated catalysts were impregnated with methyl methacrylate and, after polymerization of the latter, which takes about 48 hr, ultrathin sections were prepared from which high-resolution transmission pictures could be obtained easily.* Besides in the usual way, hydrogen adsorption was also measured by elution of the adsorbed hydrogen by means of deuterium and determination of the amount of (protium) hydrogen released. Hydrogen was adsorbed at 195°K and about 1 mm Hg. The surface area occupied by a hydrogen atom was taken to be 6.7 Å$^2$ (*6*). The results obtained by both methods agree within experimental error.

## Results and Discussion

### *A. Properties of the Reduced Catalysts*

The total surface area of the catalysts, as determined from the extent of nitrogen adsorption, and the free metal surface area, as measured by hydrogen adsorption, are given in Table 1. The values for the mean

* The authors are much indebted to Mr. A. M. Kiel of this laboratory, who developed this method and carried out the electron microscopic investigations.

TABLE 1
PROPERTIES OF THE CATALYSTS REVEALED BY ADSORPTION MEASUREMENTS

| Catalyst | Nickel content (%) | Reduction temp. (°C) | Total surface area ($m^2$/g cat) | Nickel surface area ($m^2$/g Ni) | Mean cryst. size $\bar{d}_{vs}$ (Å) |
|---|---|---|---|---|---|
| Homogeneous | 40.9 | 350 | 241 | 82 | 82 |
| precipit. | 35.4 | 350 | 208 | 105.5 | 64 |
| Harshaw | 58.5 | 350 | 125 | 77 | 90 |
| Ni-0104 P | | 450 | 92 | 62 | 109 |

particle diameter, $\bar{d}_{vs}$, calculated from $\bar{d}_{vs} = 6\ V/S$, where $V$ is the total volume of the metal in the catalyst and $S$ is the free metal surface area, are indicated in the last column of this Table. These values are compared with those obtained from X-ray line-broadening and from electron micrographs in Table 2. As appears from the figures given under the headings $\bar{d}_{vs}$ (1) and $\bar{d}_{w}$ (3) of Table 2, the particle sizes calculated from the free metal surface area found by hydrogen adsorption exceed those obtained from X-ray line-broadening about by a factor of 2. The observations of the electron microscope confirm the values found by X-ray line-broadening. Figure 1 shows a photograph of the pure support material of the homogeneously precipitated catalysts (Degussa "aerosil" 150). Figure 2 represents a photograph of the homogeneously precipitated nickel-on-silica catalyst with 35.4% nickel; it appears that the support of these catalysts is covered with very small nickel particles. The largest nickel particles that can be discerned in this and other photographs have diameters of about 35 Å only, which is in good agreement with the value determined from X-ray line-broadening. In view of the small dimensions of the metal particles in the homogeneously precipitated catalysts, it is impossible to determine a more detailed particle size distribution from the electron micrographs. Figure 3 represents a photograph of the Harshaw nickel-on-kieselguhr catalyst that contains larger metal particles. A rough classification of the particle diameters leads to Table 3. From this distribution the mean particle dimensions (which can also be obtained from X-ray

TABLE 2
COMPARISON OF MEAN DIMENSIONS OF NICKEL-ON-SILICA PARTICLES, AS OBTAINED BY DIFFERENT TECHNIQUES[a]

| Catalyst | Nickel content (%) | $\bar{d}_{vs}$ (1) (Å) | $\bar{d}_{vs}$ (2) (Å) | $\bar{d}_{w}$ (3) (Å) | $\bar{d}_{w}$ (4) (Å) |
|---|---|---|---|---|---|
| Homogeneous | 40.9 | 82[b] | — | 40[c] | — |
| precipit. | 35.4 | 64[b] | — | 30[d]; 33[e] | — |
| Harshaw Ni-0104 R | 58.5 | 90[b] / 109[f] | 47[g] | 70[g] | 60[g] |

[a] (1) $\bar{d}_{vs}$ calculated from the free metal surface area, $S$, measured by the extent of hydrogen adsorption; $\bar{d}_{vs} = 6V/S$, where $V$ is the total volume of the metal.

(2) $\bar{d}_{vs} = \Sigma_i n_i d_i^3 / \Sigma_i n_i d_i^2$ calculated from the particle-size distribution obtained from the electron micrographs.

(3) $\bar{d}_{w}$ measured by X-ray line-broadening.

(4) $\bar{d}_{w} = \Sigma_i n_i d_i^4 / \Sigma_i n_i d_i^3$ calculated from the particle-size distribution obtained from the electron micrograph.

[b] Catalyst reduced at 350°C.

[c] Catalyst reduced at 350–370°C.

[d] Catalyst reduced at 370°C.

[e] After reduction at 370°C, sorption of oxygen and subsequent reduction again at 370°C.

[f] Reduced at 450°C.

[g] Reduced at 310°C.

TABLE 3
PARTICLE-SIZE DISTRIBUTION FOR THE HARSHAW NI-0104 P NICKEL-ON-KIESELGUHR CATALYST, AS DETERMINED FROM ELECTRON MICROGRAPHS

| Particle diameter $d$ (Å) | Number of particles |
|---|---|
| $0 < d < 35$ | 48.6% |
| $35 < d < 70$ | 50.0% |
| $70 < d < 105$ | 1.2% |
| $105 < d < 140$ | 0.2% |

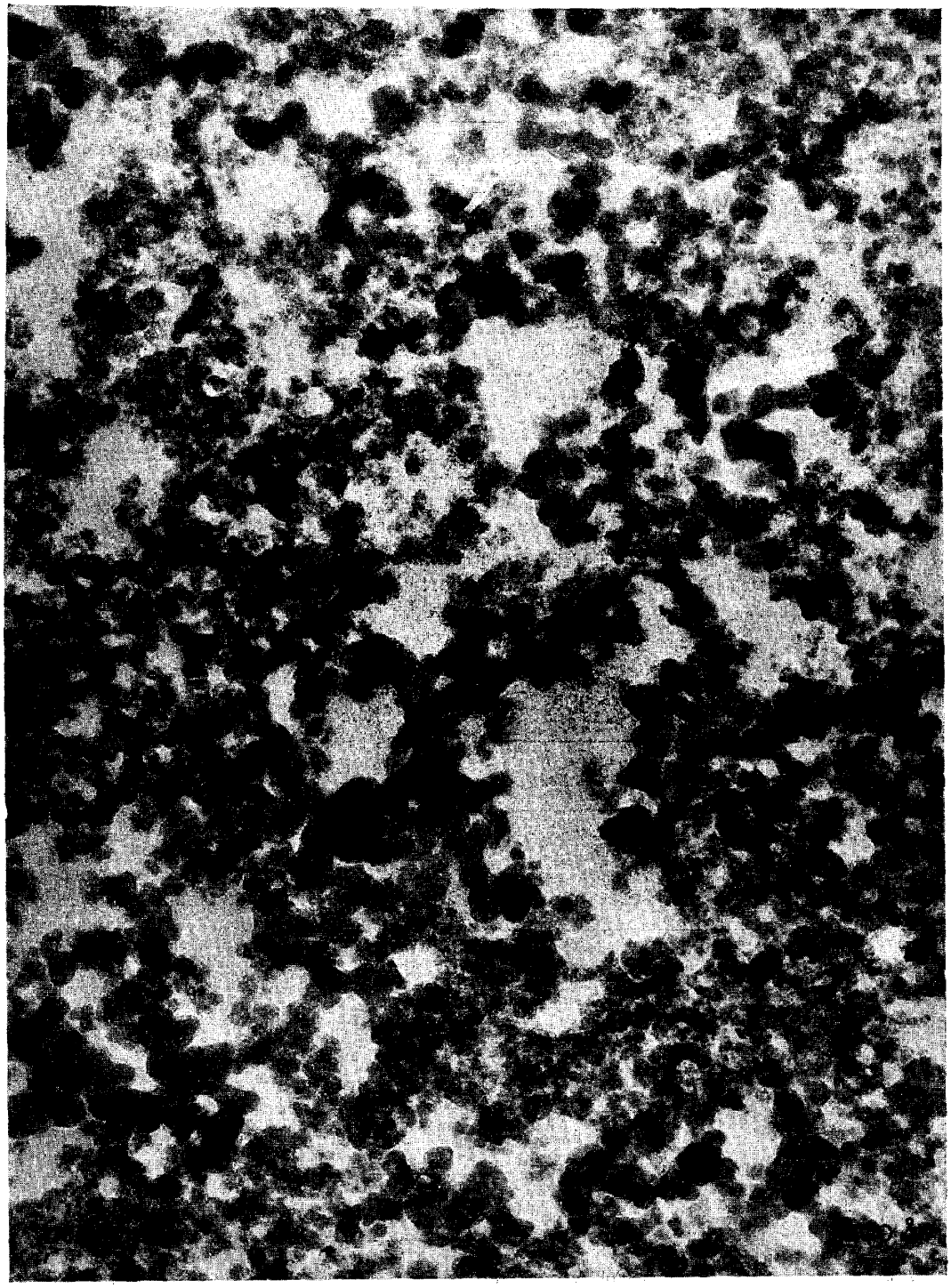

FIG. 1. Electron micrograph of pure Aerosil (Degussa 150). Sample dried at 120°C after being suspended in water and filtered. Preparation of sample: see text. Enlargement: 140 000 × (Siemens Elmiskop).


FIG. 2. Electron micrograph of a homogeneously precipitated nickel-on-silica catalyst. Nickel content: 35.4%; reduced at 370°C for 94 hr, evacuated at 370°C for 20 hr. Preparation of sample: see text. Enlargement: 140 000 × (Siemens Elmiskop).


FIG. 3. Electron micrograph of nickel-on-silica catalyst. Harshaw Ni-0104 P (58.5% nickel); reduced at 310°C for 24 hr, evacuated at 290°C for 19 hr. Preparation of sample: see text. Enlargement: 140 000 × (Siemens Elmiskop).

line-broadening and the free metal surface area, respectively) are calculated via

$$\bar{d}_w = \sum_i n_i d_i^4 \Big/ \sum_i n_i d_i^3 \quad \text{and}$$

$$\bar{d}_{vs} = \sum_i n_i d_i^3 \Big/ \sum_i n_i d_i^2$$

The resulting values are given under the headings $\bar{d}_{vs}$ (2) and $\bar{d}_w$ (4) in Table 2. The two values for $\bar{d}_w$ appear to be in fair agreement, whereas those for $\bar{d}_{vs}$ again show a large discrepancy. Inasmuch as a distribution of particle sizes is undoubtedly present in these systems, the formulas given above should give rise to a lower value for $\bar{d}_{vs}$ than for $\bar{d}_w$. This is apparent for the values calculated from the particle-size distribution of Table 3. The high value calculated from the extent of hydrogen adsorption points to the fact that the surface of the small nickel particles is not covered completely with hydrogen. This phenomenon, which is generally observed on very small nickel-on-silica particles, will be discussed thoroughly in a forthcoming publication. Presumedly it has to be ascribed to the fact that the surface of very small nickel particles is only partially accessible to gas molecules. Finally, attention is drawn to the slight increase in the mean particle size, as determined by X-ray line-broadening, from sorption of oxygen and subsequent reduction; this slight sintering will also be apparent in the magnetic measurements described below.

The nickel particles normally present in nickel catalysts are so small that no magnetic domain boundaries (*7*) are established. This implies that the magnetization in the particles is uniform, i.e., all the atomic moments are directed parallel. Magnetization of such a system of single-domain particles proceeds by orientation of the magnetic moments of the particles in an external magnetic field. In this process generally all the atomic moments of a particle rotate coherently with respect to the particle, which itself does not change its orientation. Owing to the fact that the energy varies with the orientation of the magnetic moment in the particle (ferromagnetic anisotropy), rotation of this moment requires a certain activation energy. For bulk ferromagnetics this anisotropy energy can be attributed to three sources: form anisotropy, magnetocrystalline anisotropy, and magnetostriction (*7*, *8*). For the small nearly *spherical* particles studied in this work (see the electron micrographs Figs. 2 and 3) the magnetocrystalline anisotropy is presumably the main source.

When the orientation of the magnetic moments of a single-domain particle system reaches its thermodynamic equilibrium distribution, the system is said to be superparamagnetic (*9*, *10*). Provided a correction is applied for the effect of temperature on the spontaneous magnetization of the particles, the equilibrium distribution, and consequently the magnetization, is governed only by $H/T$, where $H$ is the magnetic field strength and $T$ the absolute temperature. When the magnetization is effected by an alternating magnetic field, the time allowed for the system to reach thermodynamic equilibrium depends on the frequency of the magnetic field. Moreover, high fields ($H > \sim 10^4$ oe) decrease the energy barrier that impedes the reorientation of the moment of a particle. This implies that when a system is stated to behave superparamagnetically, it is necessary to specify the experimental conditions, viz., temperature, field strength, and frequency of the magnetizing field. With one exception the measurements reported here were done with alternating fields of 50 c/sec. The maximum RMS field strength was about 450 oe. Figure 4 gives the magnetization as a function of $H/T$ for the 40.9% homogeneously precipitated nickel catalyst reduced at 320°C. The data are corrected for the variation in the spontaneous magnetization by multiplication with $(M_{s_0}/M_{s_T})^2$, where $M_{s_0}$ is the spontaneous magnetization at 0°K and $M_{s_T}$ the spontaneous magnetization at $T$ °K. From the results shown it appears that in the range 157° to 373°K the value of the magnetization is determined only by $H/T$; this implies that in this temperature range and at this frequency the system behaves completely superparamagnetically. At higher temperatures (e.g., at 478°K) the experimental points fall below the curve. Probably this is caused

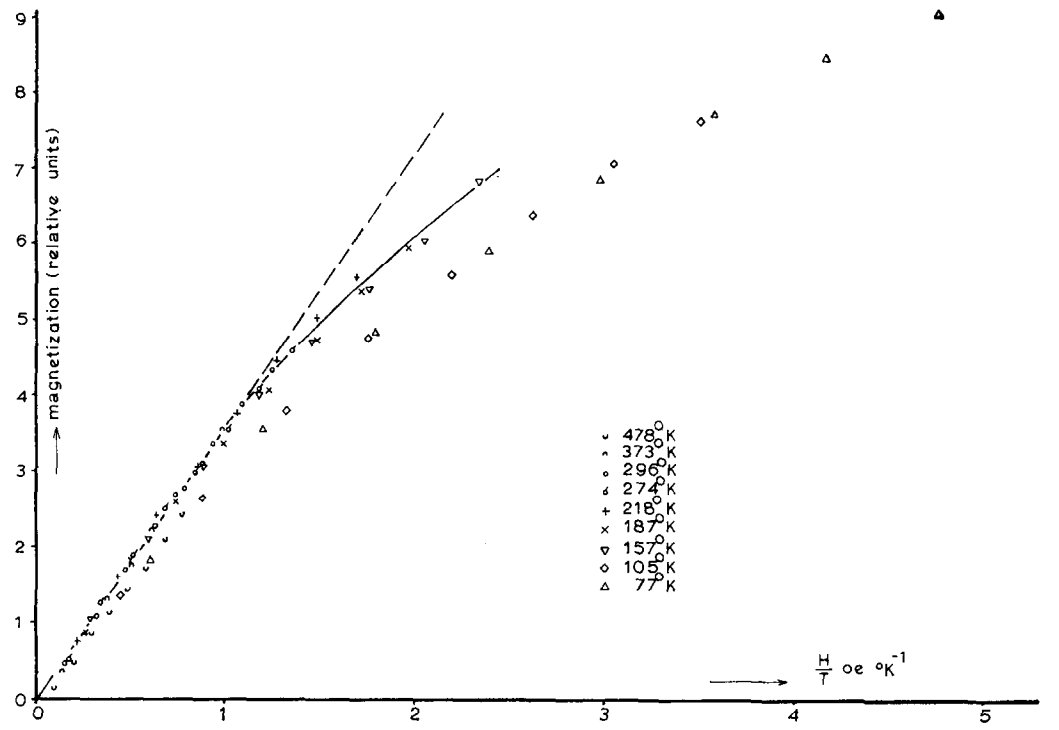


FIG. 4. Magnetization as a function of $H/T$ (field strength/absolute temperature) for a homogeneously precipitated nickel catalyst. Nickel content: 40.9%; reduced at 320C° for 62 hr, evacuated at 295°C for 19 hr.

by a slight decrease of the Curie temperature of the small nickel particles present here. Earlier this was found by Abeledo and Selwood (*11*).

It appears that below 157°K the experimental points are also lower than those measured at 157° to 373°K. This behavior is brought about by the fact that at temperatures below 157°K part of the nickel particles can no longer reach their equilibrium magnetization in about $10^{-2}$ sec.* The system does not behave superparamagnetically in this temperature range. The theoretical considerations of Néel (*12*, *13*, *14*) enable us to gain an impression of the ferromagnetic anisotropy energy involved here from the experimental deviation from superparamagnetic behavior. For the magnetization, $M$, observed $t$ sec after the establishment of the magnetizing field the following equation may be derived:

$$M = M_e\{1 - \exp(-t/\tau)\}$$

$M_e$ is the thermodynamic equilibrium magnetization, and $\tau$ is the relaxation time, given by

$$\tau = \tau_0 \exp(E_a/kT)$$

$E_a$ is the anisotropy energy per nickel particle, $kT$ has its usual meaning, and $\tau_0$ is a characteristic time estimated by Néel to be about $10^{-9}$ sec. The relaxation time, $\tau$, depends strongly on the measuring temperature, and on the value of $E_a$, which varies with the dimensions of the particle. The deviation from complete superparamagnetism does not increase on decreasing the temperature from 105° to 77°K (Fig. 4); obviously the particle-size distribution is such that a certain range of particle sizes is absent.

Now we shall compare the anisotropy

* Here the 50 c/sec alternating field is approximated by an alternating field of a rectangular form which works $10^{-2}$ sec per period in either direction.

energy of the larger particles, which can be calculated from the deviation from superparamagnetism, with that to be expected from the bulk magnetocrystalline anisotropy energy. The data of Fig. 4 suggest an anisotropy energy, $E_a$, of $3.0 \times 10^{-13}$ erg/particle. This leads to a relaxation time of $10^{-3}$ sec at 157°K; the magnetization after about $10^{-2}$ sec is equal to the thermodynamical equilibrium value under these conditions. At 105°K a relaxation time of 1 sec, is found from the $E_a$ value assumed, and the magnetization is $10^{-2}$ times the equilibrium magnetization. At 77°K these values are $2 \times 10^{+3}$ sec and $5 \times 10^{-6}$, respectively. Hence, this value for $E_a$ is in accordance with the behavior shown in Fig. 4. If *only* the same magnetocrystalline anisotropy energy as in bulk nickel is present, an anisotropy energy of $0.7 \times 10^{-13}$ erg/particle for particles with a diameter of 60 Å is calculated from the bulk anisotropy energy in this temperature range, viz. $6.5 \times 10^5$ erg/cm$^3$ (*15*). (The lowest energy barrier between two orientations of the magnetization that correspond to minimum energy is about $\frac{1}{4}$ $K_1$ per unit volume, where $K_1$ is the first anisotropy constant.) Since 60 Å is an upper limit for the particle size as found electron microscopically, the predicted value is much lower than that observed experimentally; evidently other types of anisotropy play a part.

An analogous conclusion is arrived at if we look at the results found with the Harshaw catalyst (Fig. 5). In accordance with the abovementioned presence of larger particles in this sample, deviation from superparamagnetic behavior already occurs at about 400°K. From the deviation at room temperature an anisotropy energy, $E_a$, of $6.7 \times 10^{-13}$ erg/particle is calculated in the same way as above. The bulk value for the anisotropy energy at room temperature, viz., $5 \times 10^4$ erg/cm$^3$ (*15*), gives an anisotropy energy of only $7.2 \times 10^{-14}$ erg/particle for particles with a diameter of 140 Å (the largest particle size found electron microscopically). These results suggest that the main contribution to the anisotropy of the

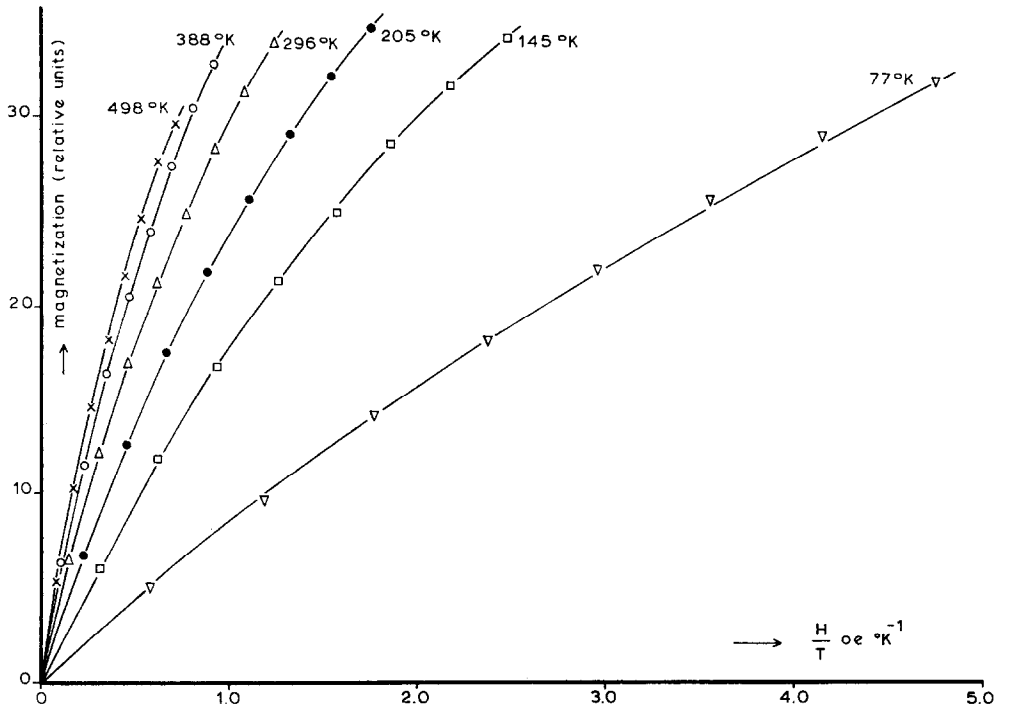


FIG. 5. Magnetization as a function of $H/T$ (field strength/absolute temperature) for nickel-on-silica catalyst Harshaw Ni-0104 P (58.5% nickel); reduced at 360°C for 39 hr, evacuated at 330°C for 18 hr.

small nickel particles studied originates from the surface. However, if the very rough theoretical estimate of 1 erg/cm$^2$ (*16*) for the surface anisotropy is accepted, rather high values are obtained, viz., $1.1 \times 10^{-12}$ and $6.2 \times 10^{-12}$ erg/particle for particles with a diameter of 60 Å and 140 Å, respectively. (In a forthcoming paper we shall discuss measurements at varying temperatures and different magnetizing frequencies which will give more information about the ferromagnetic anisotropy of small nickel particles.)

### *B. Effect of Oxygen Sorption on the Magnetization of Superparamagnetic Nickel Particles*

Chemisorption may affect the magnetization of small nickel particles in three different ways (Fig. 6):

(i) The atomic magnetic moments of the nickel surface atoms involved in the chemisorption are increased, while the exchange energy that is responsible for the ferromagnetic ordering of the atomic moments remains substantially higher than the thermal energy. Then the direction of the larger atomic moments of the metal surface atoms is still in line with the magnetization of the nickel particle. In this case an increase in magnetization will be found after chemisorption.

(ii) The atomic moments of the nickel surface atoms involved in chemisorption are decreased, while they remain ferromagnetically coupled to the other atomic moments of the particle. Now a decrease in magnetization will be found.

(iii) The atomic moments of the nickel surface atoms are increased or decreased by the chemisorption, while this process moreover causes the exchange energy of the bond between surface and subsurface nickel atoms to be decreased to well below the thermal energy. As a result the chemisorbing nickel surface atoms get into a paramagnetic or antiferromagnetic state. At low coverages, when the adsorbed atoms or molecules are far apart, presumably a paramagnetic surface state will be present. In that case, the thermal disordering of the paramagnetic atomic moments is so effective at the temperatures and magnetic field strengths used that a very small fraction of their saturation

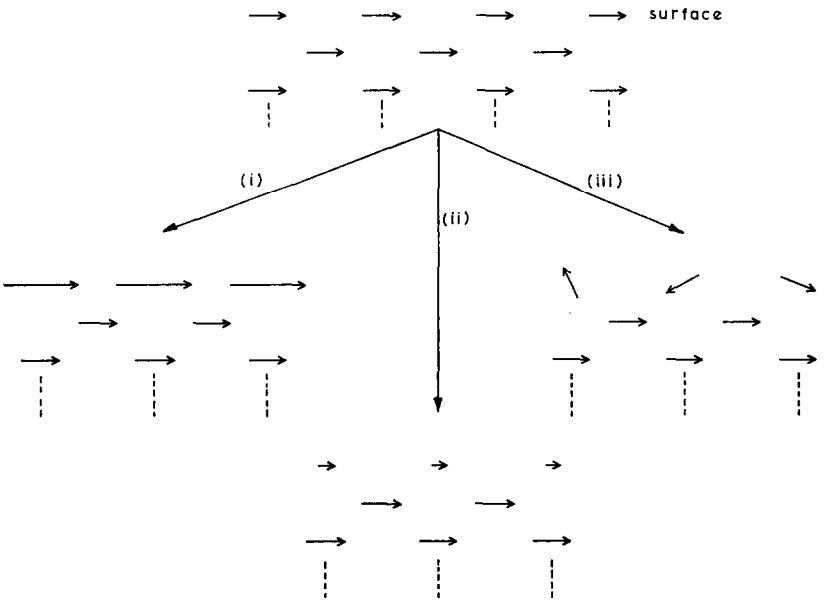


FIG. 6. Mechanisms by which chemisorption may affect the ferromagnetism of the adsorbent.

magnetization remains. This fraction of the saturation magnetization $M/M_s$, measured at a temperature $T$°K in a magnetic field $H$, is $M/M_s = \mu_a H/3\,kT$; $\mu_a$ is the magnetic moment of the nickel atom after chemisorption, and $kT$ has its normal meaning. At 77°K and 400 oe and at an atomic moment of, e.g., 3 Bohr magnetons, the value of $M/M_s$ is only $3.4 \times 10^{-5}$, whereas for a surface nickel atom ferromagnetically coupled to a nickel particle of about 1000 atoms ($\mu_a$ is 0.6 Bohr magneton) the fractional magnetization is $6.8 \times 10^{-3}$. Consequently, whether the atomic moments of the nickel surface atoms increase or decrease on chemisorption, the contribution of these atoms to the magnetization measured at low fields and not extremely low temperatures will be negligible. At higher coverages there is the possibility of an exchange interaction between the ferromagnetically decoupled nickel surface atoms. For oxygen sorption this interaction will most likely lead to an antiferromagnetic ordering of the moments of the chemisorbing nickel atoms. Then the atoms in an external magnetic field are even less magnetized than paramagnetic chemisorbing nickel atoms. Consequently, chemisorption now also leads to a decrease in the magnetization. Antiferromagnetic coupling of the moments of the chemisorbing nickel atoms to the underlying ferromagnetic phase seems very unlikely, inasmuch as a shorter distance between the nickel atoms, generally a prerequisite for antiferromagnetic interaction, is not plausible.

Adsorption of molecular oxygen decreases the magnetization of completely superparamagnetic systems, as was observed earlier by Broeder, Van Reijen, and Korswagen (*2*), Leak and Selwood (*3*), and Geus, Nobel, and Zwietering (*5*). Measurements described below will confirm this. When the interaction is restricted to the surface layer, oxygen adsorption also decreases the magnetization, as will be shown below. This can be realized by adsorption of oxygen resulting from the decomposition of nitrous oxide. Since this decomposition proceeds markedly slower on nickel surfaces covered with oxygen, it is possible to cover a large fraction of the surface with a monolayer only by the use of nitrous oxide.

Hence, either (ii) or (iii) of the mechanisms mentioned above must be present. Chemical evidence is against a decrease of the magnetic moment of nickel on reaction with oxygen. In Pauling's scale the electronegativity of oxygen is 3.5, against only 1.8 for nickel. In view of this large difference formation of a covalent bond between oxygen and nickel is very unlikely, and so is the presence of a $(3d)^{10}$ configuration for the nickel in the adsorption complex. Both $Ni^+$ $(3d)^9$ and $Ni^{2+}$ $(3d)^8$ have a magnetic moment larger than that of a metallic nickel atom. When only the spin moment can be oriented in a magnetic field, magnetic moments of 1.73 and 2.83 Bohr magnetons are expected for $Ni^+$ and $Ni^{2+}$, respectively (*17*), these moments are appreciably higher than that of metallic nickel, viz., 0.6 Bohr magnetons per atom. Consequently, mechanism (iii) will be operative here; although the moments of the nickel surface atoms increase on oxygen adsorption, their contribution to the magnetization is strongly decreased on account of the decrease in exchange energy. Since $Ni^+$ is very unstable (*18*), formation of $Ni^{2+}$ seems most likely; in that case one oxygen atom should destroy the contribution to the ferromagnetism of one nickel atom on oxidation.

The origin of the exchange coupling in ferromagnetic metals is not completely clear, and an explanation of the effect of oxygen sorption on the exchange energy will therefore have to be speculative. On the basis of the $s$–$d$ theories of the exchange interaction [for a good survey see Herring's review (*19*, *20*)], a very obvious explanation may be given. In these theories the spins of the $d$ electrons of neighboring metal atoms are directed parallel, by interactions with the $s$ electrons. When the $s$ electrons are removed from the nickel surface atoms by oxygen sorption, they lose their ability to sense the orientation of the spin of the $d$ electrons of neighboring metal atoms. When, on the other hand, the exchange coupling results from a direct overlap of $d$ orbitals on neighboring metal atoms, a small increase in interatomic

distance may profoundly decrease the exchange energy. A weakening of the bond between the chemisorbing nickel atoms and the remainder of the metal, and hence an increase in interatomic distance, is obvious. The theory of direct exchange between $d$ orbitals on neighboring atoms in nickel is, however, strongly disputed in view of the results of calculations by Watson and Freeman (*21*, *22*).

To consider the experimental results more profoundly, a quantitative description of the experimental results will be developed. For a purely superparamagnetic system, when the anisotropy energy is large compared with the magnetic energy of the particles in an external field, the magnetization is given by (*10*)

$$M_0 = \langle Nn\beta\mu_B \cos\theta \tanh(n\beta\mu_B H \cos\theta/kT)\rangle_{av} \quad (1)$$

Here uniform nickel particles containing $n$ metal atoms per particle are assumed to be present. $N$ is the number of metal particles per unit volume of catalyst, $\beta$ is the number of Bohr magnetons per nickel atom, $\mu_B$ is the magnetic moment corresponding to one Bohr magneton, $H$ is the external magnetic field, and $kT$ has its normal meaning. $\theta$ is the angle between the direction of the magnetic field and the easy axes of magnetization in the particle. The average applies to $\cos\theta$, inasmuch as in the system considered the easy axes have their directions randomly distributed. For $n\beta\mu_B H$ smaller than $kT$, Eq. (1) may be approximated by

$$M_0 = N\left\langle\left\{2\frac{n^2\beta^2\mu_B{}^2H}{kT}\cos^2\theta \Big/ \left[2+\left(\frac{n\beta\mu_B H}{kT}\right)^2\cos^2\theta\right]\right\}\right\rangle_{av} \quad (2)$$

Averaging yields the following equation

$$M_0 = N\frac{n^2\beta^2\mu_B{}^2H}{kT}\left[\frac{1}{3}-\frac{1}{10}\left(\frac{n\beta\mu_B H}{kT}\right)^2+\frac{1}{28}\left(\frac{n\beta\mu_B H}{kT}\right)^4\right] \quad (3)$$

If $n\beta\mu_B H \ll kT$, this may be approximated by

$$M_0 = N\frac{n^2\beta^2\mu_B{}^2H}{3kT}\left[1-0.3\left(\frac{n\beta\mu_B H}{kT}\right)^2\right] \quad (4)$$

Table 4 gives the values of $0.3\,(n\beta\mu_B H/kT)^2$ for particles with diameters of 30 and 60 Å in an external field of 400 oe at 77° and 300°K. As appears from these values, at 300°K Eq. (4) is here allowed. For 30-Å particles and at 300°K Eq. (4) may be replaced by

TABLE 4
ENERGY RATIOS FOR SMALL FERROMAGNETIC PARTICLES[a]

| | $n\beta\mu_B H$ ($10^{-14}$ erg) | | $n\beta\mu_B H/kT$ | | $0.3(n\beta\mu_B H/kT)^2$ | |
|---|---|---|---|---|---|---|
| | 30 Å | 60 Å | 30 Å | 60 Å | 30 Å | 60 Å |
| 77°K | 0.29 | 2.3 | 0.27 | 2.17 | 0.027 | 1.40 |
| 300°K | | | 0.070 | 0.56 | 0.002 | 0.09 |

[a] $n$, number of nickel atoms per particle; $\beta$, number of Bohr magnetons per atom; $\mu_B$, magnetic moment of one Bohr magneton; $H$, magnetic field strength, here taken to be 400 oe.

$$M_0 = N\frac{n^2\beta^2\mu_B{}^2H}{3kT} \quad (5)$$

If this equation holds, the magnetization-versus-$H/T$ plot will be a linear curve. From Eq. (5) it is easy to derive an equation for the effect of adsorption on the magnetization. First we suppose that the admitted gas molecules are homogeneously distributed over the metal particles in the catalyst. If the atomic moments of $n_a$ nickel atoms per particle are decoupled from the ferromagnetic phase, the magnetization becomes

$$M = N\frac{(n-n_a)^2\beta^2\mu_B{}^2H}{3kT}$$

Hence,

$$\frac{\Delta M}{M_0} = \frac{M-M_0}{M_0} = -2\frac{n_a}{n}+\left(\frac{n_a}{n}\right)^2 \quad (6)$$

If $x$ cm³ of oxygen per gram of nickel are adsorbed and if, per oxygen atom, the moment of one nickel atom is decoupled

$$n_a = 5.26\times10^{-3}\,(nx)$$

This leads to

$$\Delta M/M_0 = -1.052 \times 10^{-2}x + 0.0028 \times 10^{-2}x^2 \quad (7)$$

If Eq. (5) is obeyed, the relative decrease in magnetization per cm³ of oxygen sorbed does not depend on the size of the metal particles. This is obvious since both the decrease in magnetization and the amount of oxygen adsorbed per gram of nickel are proportional to $n_a/n$.

When a distribution of particle sizes is present, it is not necessarily so that $s_i/n_i$, the ratio of oxygen atoms sorbed, $s_i$, to nickel atoms, $n_i$, for the $i$th particle is equal to the ratio of all the oxygen atoms admitted to all the nickel atoms in the catalyst. When $s_i$ is the number of oxygen atoms sorbed by the $i$th particle, which contains $n_i$ atoms, Eq. (7) becomes

$$\frac{\Delta M}{M_0} = -1.052 \times 10^{-2}x \frac{\Sigma_i n_i}{\Sigma_i s_i} \frac{\Sigma_i n_i s_i}{\Sigma_i n_i^2} + 0.0028 \times 10^{-2}x^2 \left(\frac{\Sigma_i n_i}{\Sigma_i s_i}\right)^2 \frac{\Sigma_i s_i^2}{\Sigma_i n_i^2} \quad (7a)$$

Here $5.26 \times 10^{-3}x\Sigma_i n_i$ is the total number of oxygen atoms admitted; the fraction $s_i/\Sigma_i s_i$ is sorbed by the $i$th particle. Generally* it is assumed that $s_i$ is proportional to the number of metal atoms situated in the accessible part of the surface of the $i$th particle. In that case a narrow distribution of particle sizes leads to a very small deviation from Eq. (7), whereas for a wide distribution the decrease in magnetization is expected to be much smaller, since the number of surface atoms will decrease slower than $n_i$, the total number of nickel atoms, when the particle size is decreased.

To calculate the decrease in magnetization when the admitted gas molecules are not distributed homogeneously over the metal particles, we assume that $N_1$ nickel particles have adsorbed $n_a$ oxygen atoms. $(N - N_1)$ particles still have clean surfaces then. Now the relative decrease in magnetization is

$$\frac{\Delta M}{M_0} = -\left\{2\frac{n_a}{n} - \left(\frac{n_a}{n}\right)^2\right\}\frac{N_1}{N} \quad (8)$$

If $x$ cm³ of oxygen per gram of nickel are sorbed, we get

$$\Delta M/M_0 = -5.26 \times 10^{-3}[2 - (n_a/n)]x \quad (9)$$

In contrast with the case where the distribution is homogeneous, the magnetization here decreases linearly with the amount adsorbed.

At an equal amount sorbed, $N_1 n_a = N n'_a$, where $N_1 n_a$ applies to a nonhomogeneous and $N n'_a$ to a homogeneous distribution, the value of the positive term $(N_1/N)(n_a/n)^2$ is larger than that of $(n'_a/n)^2$. At low amounts of gas uptake the decrease in magnetization is consequently less than for a homogeneous distribution. It may be that $n_a/n$, the fraction of the nickel atoms decoupled from the ferromagnetism in one step, varies with the size of the metal particles, i.e., with $n$. Then the decrease in magnetization per cm³ of oxygen adsorbed depends on the particle size, as is apparent from Eq. (9).

For larger metal particles Eq. (5) is no longer valid, and we should rely on Eq. (3). From this equation, the following formula can be derived for the decrease in magnetization:

$$\frac{\Delta M}{M_0} = -\frac{N_1}{N}\left\{2\frac{n_a}{n} - \left(\frac{n_a}{n}\right)^2\right\} \left\{1 - \frac{1}{6}(n - n_a)^2\left(\frac{\beta\mu_B H}{kT}\right)^2\right\} \quad (10)$$

When the adsorption proceeds homogeneously over all the metal particles $(N_1 = N)$, the decrease in magnetization differs from that given in Eq. (6) by a factor smaller than unity. This factor gradually increases with increasing coverage of the metal, that is increasing $n_a$. At 300°K and an external

* Another possibility may be that the sticking probability of incident gas molecules is smaller for smaller metal particles. When the metal particles are mechanically weakly coupled to the support, the energy of the incident gas molecules cannot be removed quickly, which considerably decreases the efficiency of the energy transfer, and hence the sticking probability (*23*). When the particles are very small (containing some dozens of atoms) the sticking probability, and consequently the amount adsorbed, may be proportional to $n_i$, the number of atoms. However, when the particles are larger, it is not likely, especially at higher coverages, that the sticking probability will determine the amount adsorbed. Moreover, the possibility that gas molecules migrating over the surface of the support are adsorbed on the metal particles may reduce the importance of the sticking probability.

field strength of 400 oe the correction factor does not differ from unity for 30-Å particles; for 60-Å particles it varies from 0.95 to 0.97, and for 70-Å particles from 0.87 to 0.91. For a nonhomogeneous distribution of the gas molecules the value of $n_a/n$ is constant and so will be the correction factor. In both cases a lower correction factor, and therefore a smaller decrease in magnetization, must be expected at increasing particle sizes.

If the decreases in magnetization observed experimentally are to be compared with those predicted from Eqs. (7), (9), and (10), the amount of oxygen adsorbed per gram of metallic nickel, $x$, has to be calculated. For this purpose the degree of reduction of the nickel in the catalyst has to be known. As explained under the heading "Materials," the homogeneously precipitated catalyst is completely reduced after reduction at 370°C for 72 hr. As only this catalyst is completely superparamagnetic at room temperature, the considerations of the effects of oxygen sorption on the magnetization have to be restricted to this catalyst. As mentioned above, the catalyst reduced at 370°C contains nickel particles of around 35 Å. Figure 7 gives the magnetization-versus-$H/T$ plot measured at 296° and 77°K. For the experimental points measured at 296°K the deviation from linearity is very small. From this and from the mean particle size it may be expected that either Eq. (7) or Eq. (9) is obeyed.

When nitrous oxide is decomposed on nickel, the reaction proceeds relatively slowly (*24*). Because it may be expected that the transport of the gas admitted through the pores of the catalyst system will be faster than the decomposition, a homogeneous distribution of the oxygen atoms over the nickel particles is likely. Consequently a description by Eq. (7) is to be expected. Figure 8 gives a comparison of the experimental decreases in magnetization for adsorption of oxygen from nitrous oxide with those predicted by Eq. (7) for a 35.4% nickel catalyst reduced at 370°C. It appears

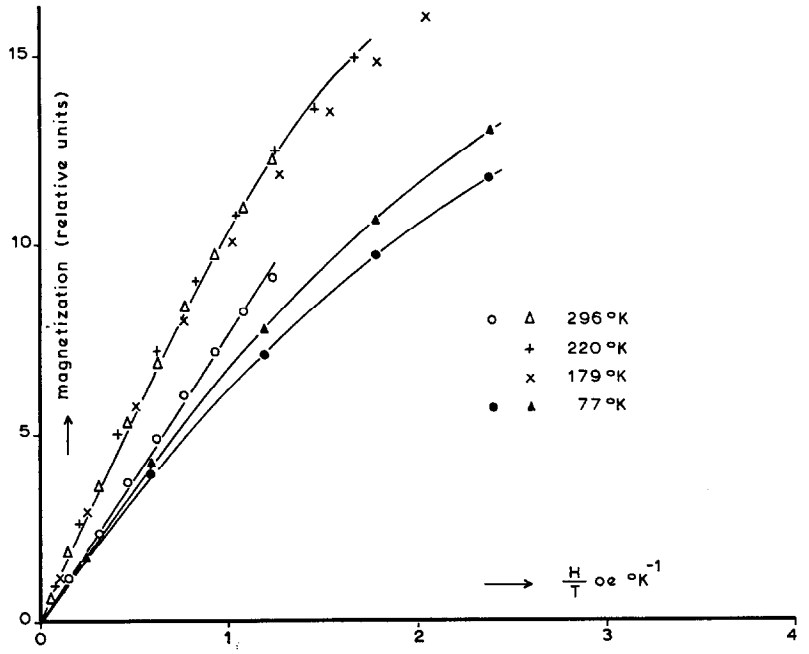


FIG. 7. Magnetization as a function of $H/T$ (field strength/absolute temperature) for a homogeneously precipitated nickel-on-silica catalyst. Nickel content: 35.4%; ○, ●, reduced at 370°C for 70 hr, evacuated at 360°C for 22 hr; △, +, ×, ▲, same catalyst subjected twice to oxygen sorption, reduction, and evacuation at 360°C.

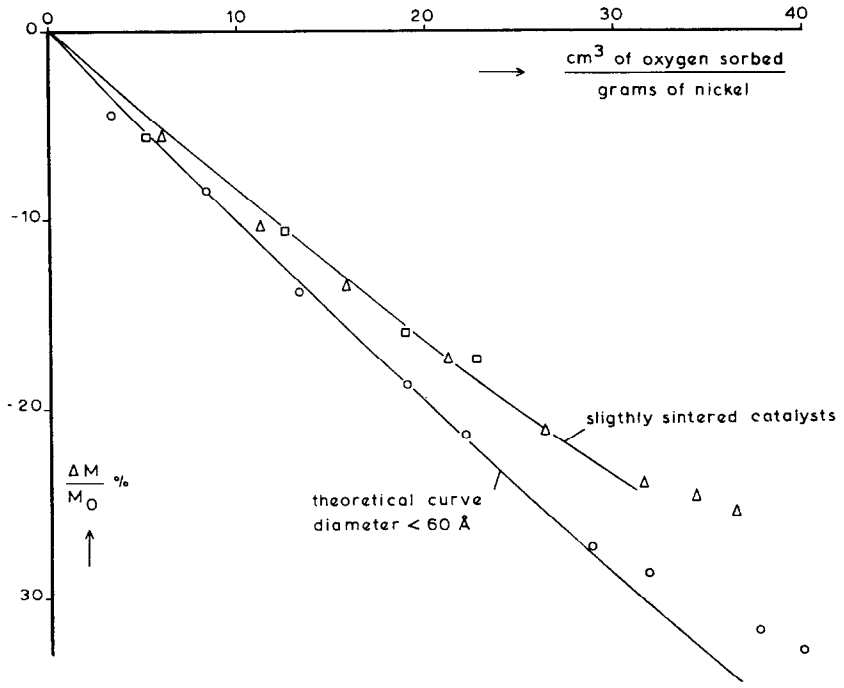


FIG. 8. Decrease in magnetization by adsorption of oxygen from nitrous oxide measured at 296°K; homogeneously precipitated nickel catalyst; ○, nickel content of 35.4%, reduced at 370°C for 70 hr; evacuated at 360°C for 22 hr; △, same catalyst subjected twice to oxygen sorption, reduction, and evacuation; □, catalyst with nickel content of 40.9%, after reduction at 320°C for 25 hr, reduced at 440°C for 25 hr and evacuated at 440°C for 20 hr. Curve calculated theoretically for particles with diameters smaller than 60 Å.

that the experimental points agree, within experimental error, with the theoretical curve. Evidently the factors

$$\frac{\Sigma_i n_i}{\Sigma_i s_i}\,\frac{\Sigma_i n_i s_i}{\Sigma_i n_i^2} \quad \text{and}$$

$$\left(\frac{\Sigma_i n_i}{\Sigma_i s_i}\right)^2 \frac{\Sigma_i s_i^2}{\Sigma_i n_i^2} \text{ of Eq. (7a)}$$

are about unity. Since a rather wide distribution of particle sizes is present in these catalysts, as appeared from the magnetic properties (Fig. 4), this implies that the very small nickel particles adsorb oxygen to a limited extent as compared with the number of surface atoms to be expected. Hence, it may be concluded that the inaccessibility of a considerable part of the surface to gas molecules is confined to very small nickel particles.

At adsorptions of more than about 30 cm³ of oxygen per gram of nickel, however, the decrease in magnetization is smaller than is theoretically expected. As may be concluded from the surface area calculated from the extent of hydrogen adsorption for this catalyst (Table 1), 30 cm³ of oxygen per gram of nickel corresponds to $1.7 \times 10^{15}$ oxygen atoms per cm². Therefore, the accessible surface is covered almost completely. The smaller effect on the magnetization observed here, may be ascribed to a concurrent slow decomposition of nitrous oxide on active spots on the fresh nickel oxide already generated by chemisorption and subsequent adsorption of the oxygen formed on these sites. This causes some of the bivalent nickel ions to be converted into trivalent ions, which does not affect the magnetization as measured. The slow decomposition of nitrous oxide on nickel oxide was demonstrated by Rudham and Stone (*25*) by means of calorimetric measurements.

When after adsorption of oxygen the homogeneously precipitated catalyst is reduced again at 370°C, some sintering of the nickel particles occurs, as was mentioned

earlier. This is also evident from the magnetization-versus-$H/T$ plot, which is also given in Fig. 7. As appears from this graph, the magnetization, which is proportional to $\Sigma_i n_i^2$, is markedly higher now. Therefore, an effect of the increased particle size on the decreases in magnetization must be expected. In Fig. 8 also the effect of oxygen sorption from nitrous oxide on the magnetization of the slightly sintered catalyst is given. As is predicted by Eq. (10), the decreases in magnetization are now clearly smaller than those for the unsintered catalyst. The same figure gives the data for the homogeneously precipitated catalyst containing 40.9% nickel after reduction at 450°C. Evidently this catalyst contains nickel particles with diameters of the same order of magnitude as those in the oxidized and reduced catalyst with 35.4% nickel, since the experimental points coincide well in both cases.

When the 40.9% nickel catalyst is reduced at 310°C, it contains very small nickel particles, as is evident from the data in Fig. 4. However, the thermogravimetric results show that the nickel is not completely reduced at this temperature. There remains some nickel in the oxide phase, which does not absorb oxygen and does not contribute to the magnetization as measured. This causes the values for $x$, the amount of oxygen adsorbed per gram of nickel, calculated from the total amount of nickel in the catalyst to be too low. If it is assumed that by reduction at 310°C 86% of the nickel in the catalyst is reduced to the metal, while this value does not change after adsorption of oxygen and subsequent reduction, the data of Fig. 9 are obtained. These data coincide with the theoretically calculated curve within the experimental error, just as in Fig. 8.

It is known that oxygen from molecular oxygen is sorbed instantaneously by nickel surfaces, till more than a monolayer of oxide has formed (*24*, *26*). Therefore, it must be expected that the transport of the oxygen through the catalyst pores is slower than the sorption. This leads to a nonhomogeneous

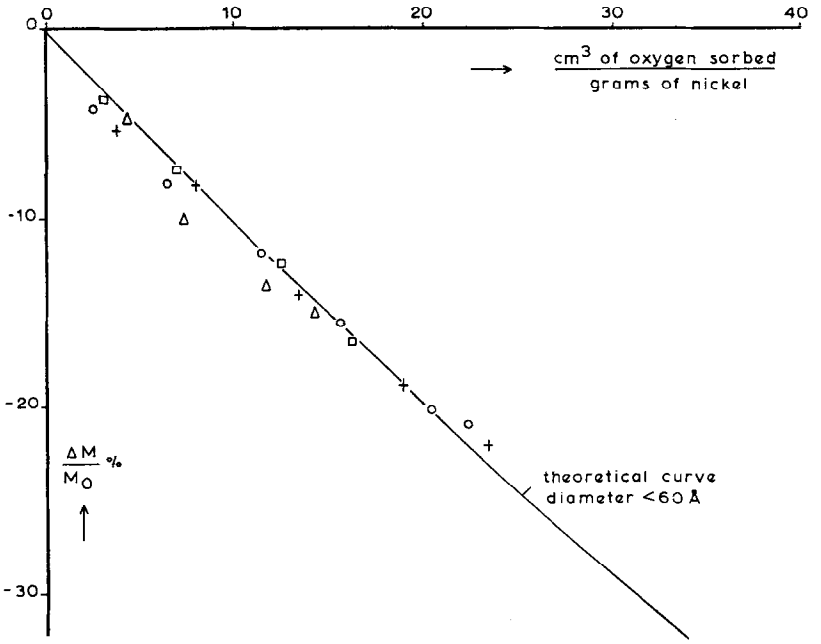


FIG. 9. Decrease in magnetization by adsorption of oxygen from nitrous oxide measured at 296°K. Homogeneously precipitated nickel catalyst (40.9% nickel) reduced at 320°C for 62 hr, evacuated at 295°C for 19 hr; □, not subjected; ○, subjected once; △, subjected five times; and +, subjected seven times to oxygen sorption, reduction and evacuation. Catalyst not completely reduced; a degree of reduction of 86% is assumed. Curve calculated theoretically for particles with diameters smaller than 60 Å.

distribution of the oxygen molecules over the nickel particles. Only in the very first stage of the adsorption process for the particles situated on the outside of the catalyst pellets may a gradual increase in coverage be expected. Figure 10 shows the decreases in phase. Exactly the same behavior was found by Leak and Selwood (*3*).

Substitution of the experimental data in Eq. (9) gives $n_a/n$ values of about 0.6. This implies that the nickel particles are oxidized for about 60% in one step. Evidently this

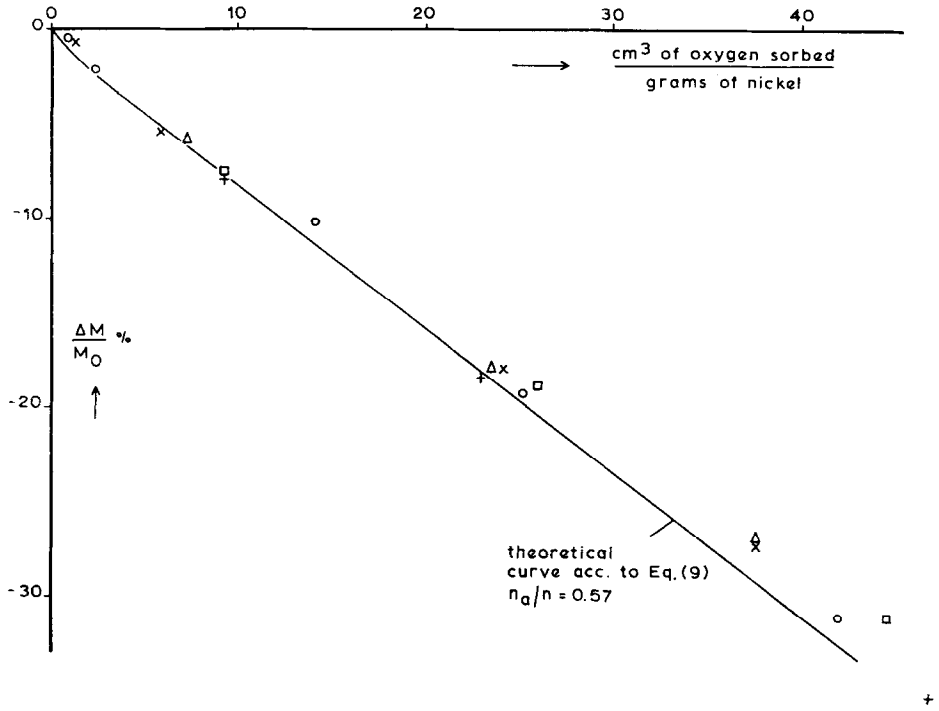


FIG. 10. Decrease in magnetization by sorption of oxygen from molecular oxygen measured at 296°K. Homogeneously precipitated nickel catalysts: *40.9% nickel catalyst* reduced at 310°C for 70 hr, evacuated at 350°C for 22 hr: +, subjected twice; □, subjected five times to oxygen sorption and reduction. Assumed degree of reduction: 86% *35.4% nickel catalyst:* ○, reduced at 370°C for 70 hr, evacuated at 350°C for 22 hr, and subjected once to oxygen sorption, reduction, and evacuation; △, reduced at 370°C for 70 hr, evacuated at 350°C for 22 hr, and subjected three times to oxygen sorption, reduction, and evacuation; ×, reduced at 350°C for 137 hr, evacuated at 350°C for 16 hr.

magnetization brought about by sorption from molecular oxygen for the homogeneously precipitated catalysts. The data for the catalyst reduced at 310°C are calculated on the assumption that the degree of reduction is 86%, which was concluded from the nitrous oxide results. After adsorption of some 3 cm³ of oxygen the magnetization decreases linearly with the amount sorbed. As mentioned above, the initial deviation from linearity is caused by a more homogeneous distribution of the oxygen over the particles easily accessible from the gaseous is an average over the particle-size distribution. It is likely that the smaller particles are oxidized more than the larger ones. The magnetization-versus-$H/T$ plots belonging to the catalysts reduced at 370°C are shown in Fig. 11. As appears from these data, the particle size is slightly increased by reduction subsequent to oxygen sorption. The data of Fig. 10 indicate that the magnetization of the slightly sintered catalyst (open squares) is decreased relatively less on oxygen sorption. This is due to a further oxidation, since the values for the correction

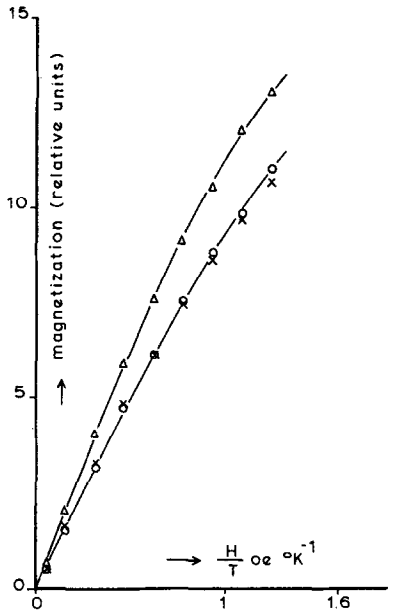


FIG. 11. Magnetization as a function of $H/T$ (field strength/absolute temperature) for a homogeneously precipitated nickel-on-silica catalyst (35.4% nickel): ×, reduced at 350°C for 137 hr, evacuated at 350°C for 16 hr; ○, reduced at 370°C for 70 hr, evacuated at 350°C for 20 hr, and subjected once to oxygen sorption, reduction, and evacuation; △, reduced at 370°C for 70 hr, evacuated at 350°C for 20 hr, and subjected three times to oxygen sorption reduction, and evacuation.

factor in Eq. (10) remain close to unity at the high values of $n_a/n$ present here. Presumably the further oxidation is caused by the somewhat larger distances between the metal particles on the supporting material after sintering.

To conclude this section, the assumption used in the interpretation of the results, viz., one oxygen atom destroys the ferromagnetism of one nickel atom, will be considered more closely. Although the experiments are quantitatively well accounted for by this assumption, the presence of a distribution of particle sizes makes this interpretation not completely unambiguous. However, it can be concluded from the results that the effect on the magnetization per oxygen atom taken up is the same both on adsorption and on further oxidation, which occur on interaction with nitrous oxide and molecular oxygen, respectively. As was argued above, the differences in the experimental curves, when sorption occurs from nitrous oxide or molecular oxygen, can be ascribed to a different distribution of the sorbed atoms only. More evidence pointing to homogeneous adsorption up to about monolayer coverage from nitrous oxide and heterogeneous further oxidation from molecular oxygen will be given in the next section. Inasmuch as on further oxidation one oxygen atom is known to react with one nickel atom, it necessarily follows that also when the interaction is restricted to a monolayer, one nickel atom will bind one oxygen atom. The same conclusion can be drawn from the work of Lewis (*27*) on the effect of oxygen sorption on the K X-ray absorption edge of nickel. Since this author used molecular oxygen in his experiments, however, the possibility of a further oxidation from the beginning is not excluded.

Finally it should be remarked that, according to the explanation given above, measurements of the effects of oxygen sorption on the ferromagnetic moment indicate only the decoupling of the moments of nickel surface atoms from the ferromagnetism. The state of the nickel atoms after chemisorption is not revealed here. Therefore, a difference between nickel ions binding chemisorbed oxygen ions and those present in nickel oxide is still compatible with the above results. It may be expected that formation of nickel ions in the surface layer of the metal should lead to a reconstruction of this layer. Low-energy electron-diffraction results of MacRae (*28*) clearly point to a displacement of an increasing fraction of the metal surface atoms with increasing coverage.

### *C. Effects of the Sorption of Oxygen on the Apparent Magnetization of Systems That Do Not Behave Completely Superparamagnetically*

Figure 12 is the magnetization-versus-$H/T$ plot for the homogeneously precipitated catalyst, both after reduction at 370°C only and subjected three times to oxygen sorption and reduction. Points measured at 77° and 296°K are given. As mentioned above, the magnetic moments of part of the nickel

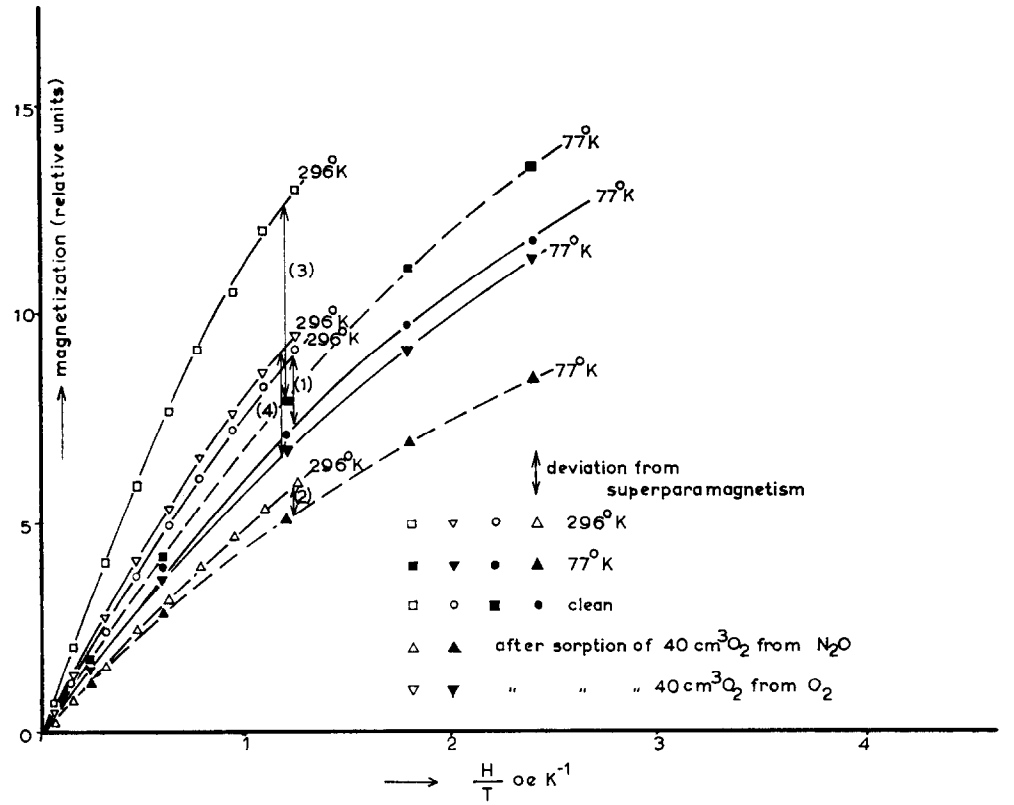


FIG. 12. Effect of sorption from nitrous oxide and from molecular oxygen on the deviation from superparamagnetic behavior at 77°K. Homogeneously precipitated nickel-on-silica catalyst (35.4% nickel): ○, ●, reduced at 370°C for 70 hr, evacuated at 350°C for 22 hr; □, ■, subjected three times to oxygen sorption, reduction, and evacuation; (1), deviation before and (2) deviation after adsorption of about 40 cm³ of oxygen from nitrous oxide; (3) deviation before and (4) deviation after sorption of about 40 cm³ of oxygen from molecular oxygen.

particles cannot follow the variations of the magnetizing fields at 77°K. Figure 12 also shows the data for the catalysts after sorption of 40 cm³ of oxygen per gram of nickel from nitrous oxide and from molecular oxygen, respectively. After reduction at 370°C, the deviation from superparamagnetic behavior was about 19% at 77°K; after adsorption of oxygen from nitrous oxide this deviation appeared to have decreased to 10%. After the catalyst had been subjected three times to adsorption of oxygen and subsequent reduction, the deviation from superparamagnetic behavior had increased to 38% at 77°K owing to the slightly increased particle size. After sorption of 40 cm³ of molecular oxygen the deviation had decreased to 26%.

These results imply that oxygen sorption decreases not only the magnetic moments of the nickel particles, but also the ferromagnetic anisotropy energy that governs the approach to thermodynamic equilibrium of the orientation of the magnetic moments. Consequently, oxygen sorption has a twofold effect when a deviation from completely superparamagnetic behavior is present: The value of the magnetic moment of the nickel particles is reduced and part of the particles may align their magnetic moments with the magnetizing field more rapidly than before. The first effect leads to a decrease in the apparent magnetization, the second to an increase. In Fig. 13 the situation is explained by means of an imaginary experiment in which the equilibrium magnetization de-

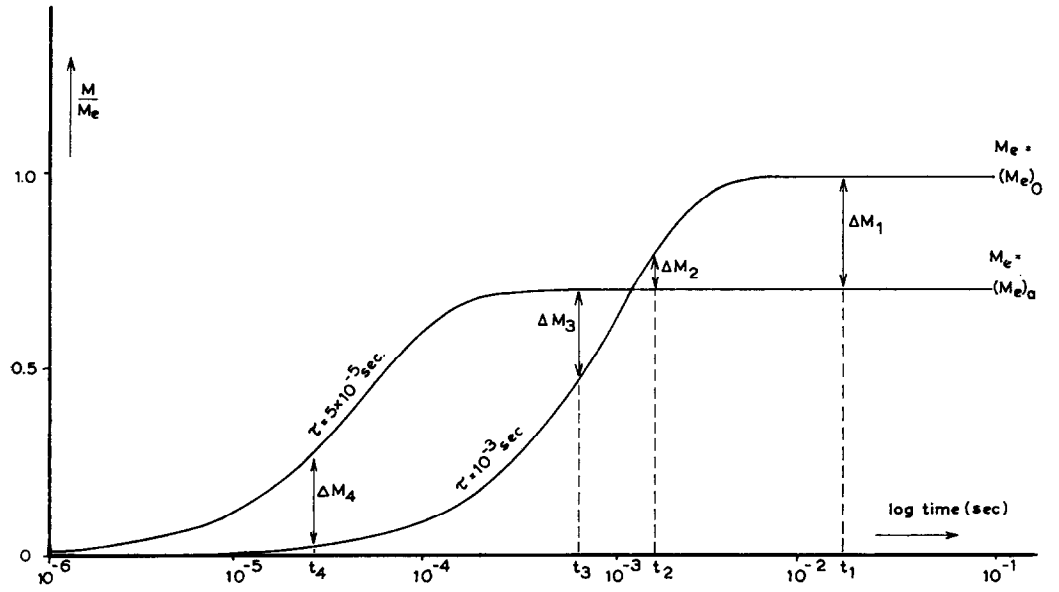


FIG. 13. Ratio of apparent magnetization ($M$) to thermodynamic-equilibrium magnetization ($M_e$) as a function of the reciprocal value of the frequency of the magnetizing field. Curves calculated according to $M/M_e = [1 - \exp(-t/\tau)]$. Oxygen sorption is supposed to decrease the equilibrium magnetization by 30%; the relaxation time, $\tau$, decreases from $10^{-3}$ sec to $5 \times 10^{-5}$ sec.

creases by 30%, on adsorption of, e.g., 40 cm³ of oxygen per gram of nickel. $(M_e)_0$ is the thermodynamic equilibrium magnetization before adsorption, $(M_e)_a$ after adsorption. After oxygen sorption the equilibrium magnetization decreases, but the equilibrium value is reached in a shorter time. If the magnetization is measured with an alternating field with a frequency of $(t_1)^{-1}$ or lower, the decrease by oxygen sorption is found to be 30%. If the frequency of the magnetizing field is $(t_2)^{-1}$, a smaller decrease in magnetization is recorded, whereas for a frequency of $(t_3)^{-1}$ or $(t_4)^{-1}$ even an increase in magnetization is measured.

Figure 14 shows the influence of oxygen sorption originating from nitrous oxide for the homogeneously precipitated catalyst. At 77°K the deviation from superparamagnetism is 20%. At this temperature the decrease in magnetization due to sorption of 26 cm³ of oxygen (from nitrous oxide) is 18% less than the decrease found at 296°K, when the system is fully superparamagnetic. It is seen from Fig. 14 that in the case of oxygen sorption from molecular oxygen practically the same results are found; here the effect is 23% less at 77°K (at this temperature the deviation from superparamagnetism was 29%) than at 296°K. Partly these smaller decreases in the magnetization measured at 77°K must be ascribed to a larger deviation from Eq. (6) at this temperature, and, consequently, a lower correction factor [see Eq. (10)].

The explanation of these influences of sorption on the ferromagnetic anisotropy is obvious. In the discussion of the magnetic behavior of our catalysts we saw that the ferromagnetic anisotropy largely resides in the surface of the small particles. On sorption of oxygen a surface layer is converted to nickel oxide and the surface area of the remaining ferromagnetic core is diminished. Consequently the anisotropy decreases.

However, if we consider experiments where the deviation from superparamagnetism is larger, a more elaborate explanation of the results is necessary. Such larger deviations may be realized, *inter alia*, in experiments with larger particles (a larger surface area per particle and hence a larger

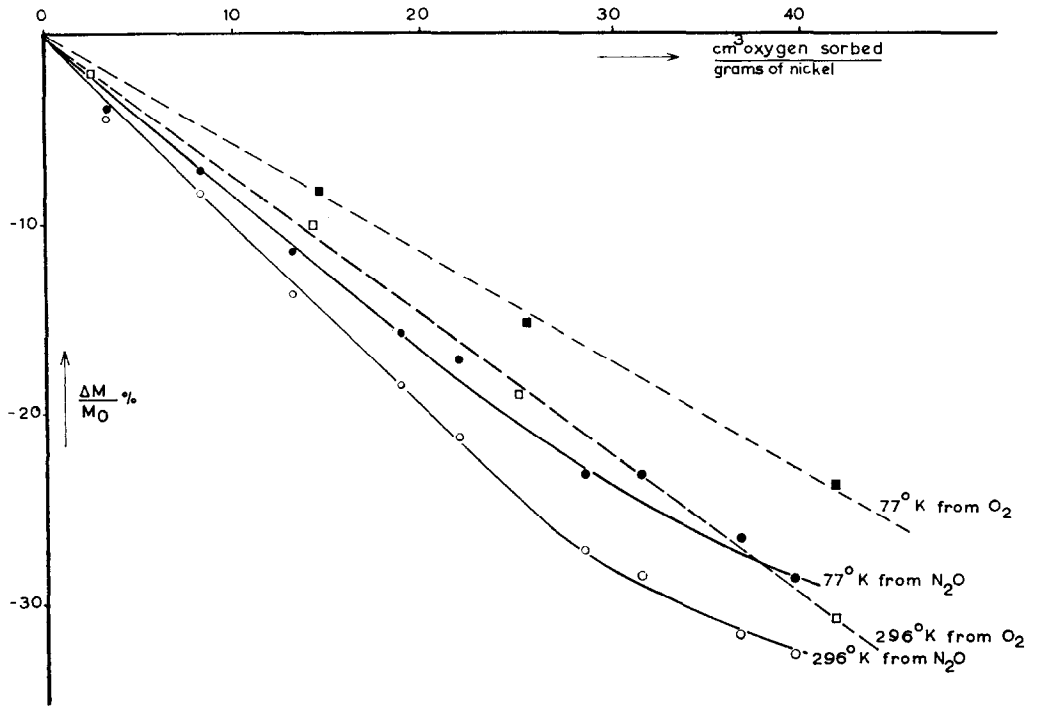


FIG. 14. Effects of sorption from molecular oxygen and from nitrous oxide on the magnetization of the homogeneously precipitated nickel-on-silica catalyst. Measurements on both completely (at 296°K) and incompletely (at 77°K) superparamagnetic systems are shown. Nickel content: 35.4%; ○, ●, reduced at 370°C for 70 hr, evacuated at 350°C for 22 hr; □, ■, same catalyst subjected once to oxygen sorption, reduction, and evacuation.

anisotropy). Figure 15 shows the situation in such a case. This figure relates to the same catalyst as discussed in Fig. 14; however, the particle size was increased by an oxidation and reduction treatment. In this case the deviation from superparamagnetism is around 38% at 77°K (compared to 20% in the former case). At 77°K the decrease in magnetization on adsorption from nitrous oxide is markedly smaller than on sorption from molecular oxygen. This trend (viz., that the points measured on adsorption from nitrous oxide lie above those found on sorption from oxygen) is more pronounced, when the metal particles, and consequently also the deviation from superparamagnetism, are still larger. The Girdler nickel-on-alumina catalyst contains much larger nickel particles after reduction at 355°C for only 20 hr. At 77°K the deviation from superparamagnetism is no less than 75%. Figure 16 is the magnetization-versus-$H/T$ plot for this catalyst. Even at 296°K the experimental points do not coincide with the points measured at higher temperatures for the same $H/T$ values. As appears from Fig. 17, in which the effects of adsorption from nitrous oxide are given, the magnetization at 77°K first increases, then traverses a maximum, and finally falls below the original value. At 296°K the magnetization steadily decreases. This behavior was studied more extensively on the Harshaw nickel-on-silica catalyst. As appears from the magnetization-versus-$H/T$ plot shown in Fig. 5, this catalyst behaves about the same as the Girdler catalyst; here, too, no complete superparamagnetic behavior is displayed at 296°K. In accordance with this the decrease at room temperature is slightly less on adsorption from nitrous oxide than on sorption from molecular oxygen, as is shown in Fig. 18. At 77°K

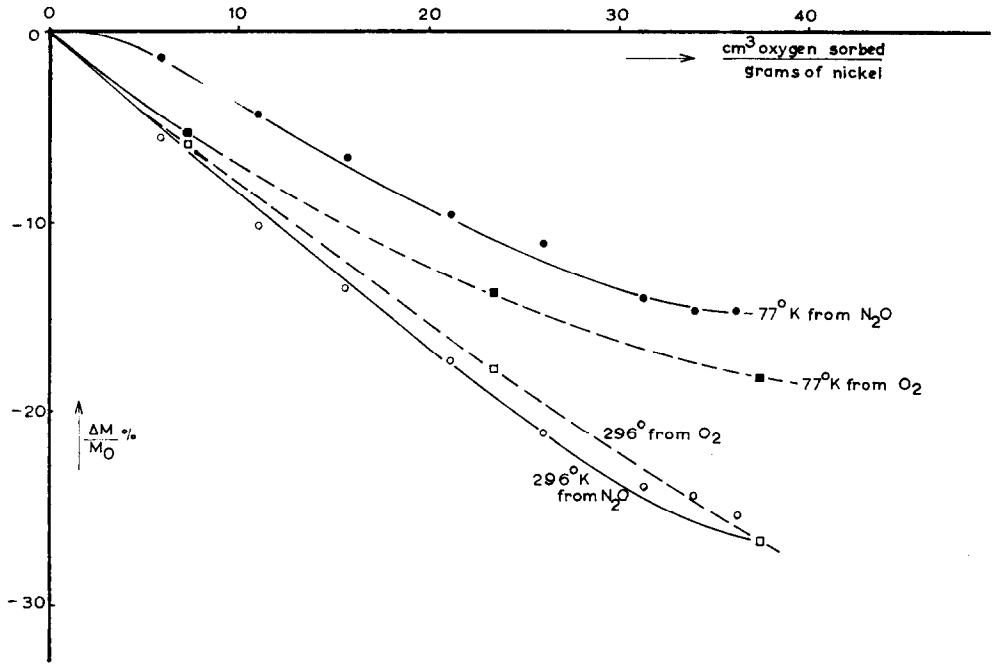


FIG. 15. Effects of sorption from molecular oxygen and from nitrous oxide on the magnetization of the homogeneously precipitated slightly sintered nickel-on-silica catalyst. Measurements on both completely (at 296°K) and incompletely (at 77°K) superparamagnetic systems are shown. Nickel content: 35.4%; reduced at 370°C for 70 hr, evacuated at 350°C for 22 hrs; ○, ●, subjected three times; and □, ■, subjected four times to oxygen sorption, reduction, and evacuation.

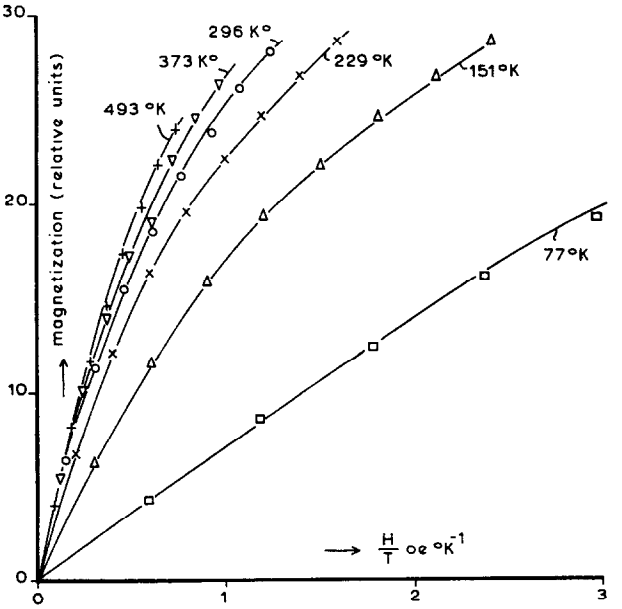


FIG. 16. Magnetization as a function of $H/T$ (field strength/absolute temperature) for the nickel-on-alumina catalyst (Girdler G-12). Nickel content: 51%. Reduced at 355°C for 19 hr, evacuated at 330°C for 19 hr (only partially reduced).

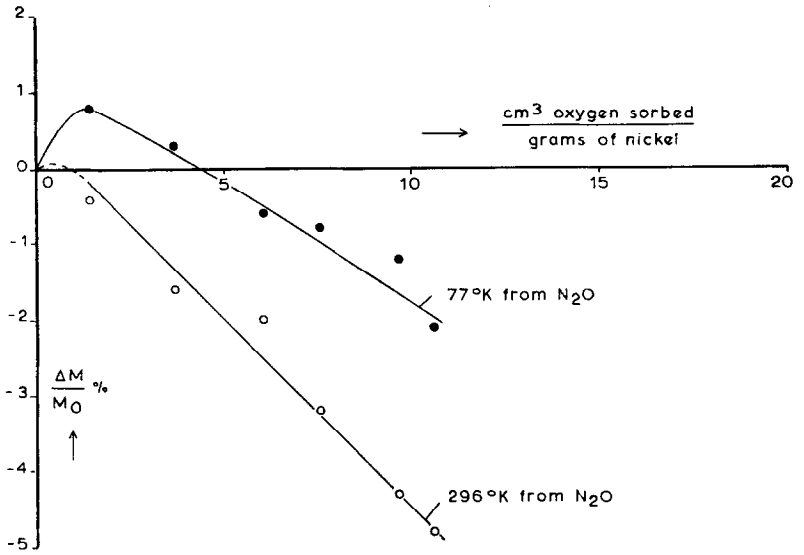


FIG. 17. Effects of sorption from nitrous oxide on the magnetization of the nickel-on-alumina catalyst (Girdler G-12, 51% nickel). Magnetization measured at 296° and 77°K. Catalyst reduced at 355°C for 19 hr, evacuated at 330°C for 19 hr (only partial reduction).

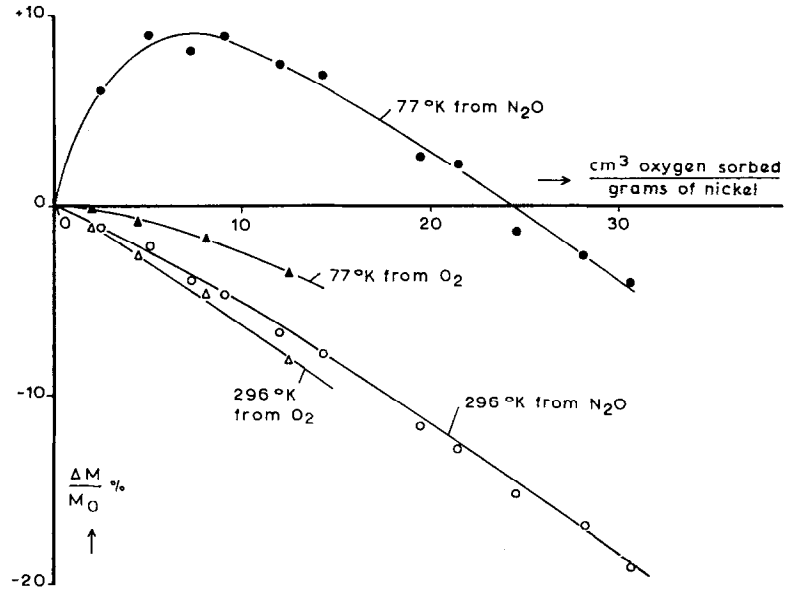


FIG. 18. Effects of sorption from nitrous oxide and molecular oxygen on the magnetization of a nickel-on-silica catalyst (Harshaw Ni-0104 P; 58.5% nickel). Magnetization measured at 296° and 77°K; ○, ●, reduced at 350°C for 72 hr, evacuated at 340°C for 23 hr; △, ▲, reduced at 360°C for 39 hr, evacuated at 340°C for 19 hr.

adsorption from molecular oxygen still decreases the magnetization, whereas adsorption from nitrous oxide strongly increases it in the first stage of the adsorption process.*

The difference in sign between the effects of adsorption from nitrous oxide at 77° and at 296°K might be ascribed to a difference in the chemisorptive bond on larger nickel

* It is apparent from Figs. 17 and 18 that here nickel particles on both silica and alumina behave in the same way. Evidently these results do not depend on the supporting material.

particles at these temperatures. This explanation is refuted, however, on the ground of measurements with magnetizing fields alternating at different frequencies. Full details of these experiments will be published elsewhere; here it may suffice to mention that the variation of the increase in self-induction of a coil, by filling it with a nickel catalyst, is determined after sorption of increasing amounts of oxygen. In these measurements the field strength is appreciably smaller. For the Harshaw catalyst the results of these measurements are given in Fig. 19. For sorption from molecular oxygen the behavior does not change very much. Both at 77° and at 296°K the magnetization decreases. At 296°K the decrease in magnetization does not vary with the frequency of the magnetizing field; the decrease is slightly smaller than that measured with higher field strengths at 50 c/sec. At 77°K the decrease is about the same as

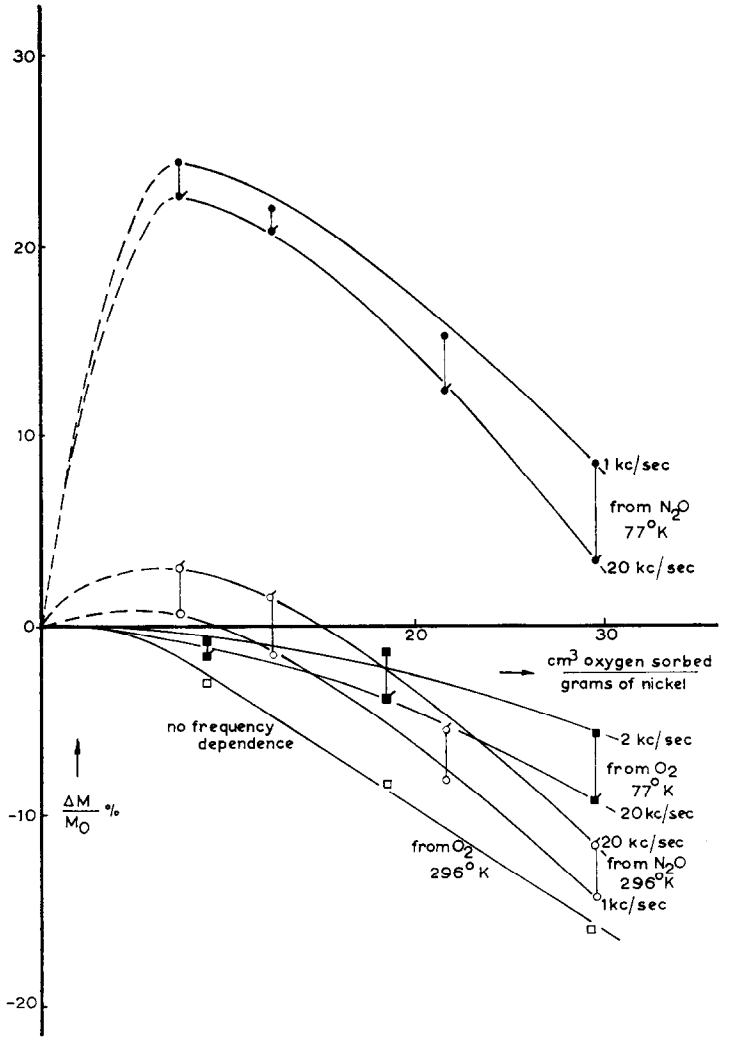


FIG. 19. Effects of sorption from nitrous oxide and molecular oxygen on the magnetization of the nickel-on-silica catalyst Harshaw Ni-0104 P, 58.5% nickel. The magnetization is measured at relatively low field strengths and varying frequencies. In the measurement of sorption from oxygen the frequency varies from 2 to 20 kc/sec, on sorption from nitrous oxide from 1 to 20 kc/sec; ○, ●, ◐, reduced at 300°C for 116 hr, evacuated at 300°C for 16 hr; □, ■, ◧, reduced at 330°C for 50 hr, evacuated at 300°C for 16 hr.

that observed at 50 c/sec (Fig. 18), but at lower frequencies the decrease is smaller than at higher frequencies. In Fig. 19 only the values observed at the highest and lowest frequencies are indicated; as the frequency is decreased from 20 kc/sec to 2 kc/sec, the decrease in magnetization becomes gradually smaller. For adsorption from nitrous oxide the difference from the 50-c/sec results is much more pronounced. Here, the magnetization first increases at room temperature, too; a maximum is then traversed after which the magnetization decreases below the original value. Here the curve obtained at the highest frequency runs above that measured at lower frequencies. The fact that also at 296°K the magnetization increases on sorption of oxygen clearly demonstrates that the increase observed at 77°K is not due to a bonding of oxygen different from that at 296°K. The results obtained at 77°K show again the same pattern of behavior; in this case a high maximum is traversed, and at high coverages the magnetization remains above the original value. Just as in the molecular oxygen measurements at 77°K, but in contrast with the nitrous oxide measurements at 296°K, the curve at the highest frequency runs below that obtained at lower frequencies.

To understand the difference in the effects of oxygen sorption from nitrous oxide and molecular oxygen, it should be realized that on sorption from molecular oxygen particle after particle is oxidized for about 60%. On chemisorption from nitrous oxide, on the other hand, homogeneous adsorption over the surfaces of the nickel particles occurs. In the latter case the equilibrium magnetization decreases gradually and so does the anisotropy energy, since the surface area of the ferromagnetic phase becomes smaller. The homogeneously precipitated catalysts, measurements on which are represented in Figs. 14 and 15, do not reach their equilibrium magnetization in 1/100 sec at 77°K. For the Girdler and Harshaw catalysts this situation is already present at 296°K. In all these cases (Figs. 14, 15, 17, and 18) adsorption from nitrous oxide steadily decreases the magnetization. This implies that the situation between $t_1$ and $t_2$ given in Fig. 13 is present here. For the first amounts of gas adsorbed the decrease in magnetization is smaller than the decrease in the equilibrium magnetization, since after adsorption equilibrium is more closely approximated. At higher coverages the anisotropy energy may be expected to be decreased so far that the magnetization reaches its equilibrium value in the time given by the reciprocal value of the frequency. In that case the incremental decreases in magnetization should be those for a superparamagnetic system. For such a system, in which the amount of oxygen adsorbed per gram of nickel increases from 20 to 30 cm³, a decrease of 7.2% is expected from Eq. (10) for particles with a diameter of 80 Å. In Fig. 18 a decrease of 7.0% is observed over the range of coverages mentioned. However, as the magnetization before adsorption ($M_0$) is lower than the equilibrium magnetization, the experimental decrease is smaller than expected. This must be ascribed to the presence of the small fraction of larger metal particles in the Harshaw catalyst. While in the later stages of the adsorption process the particles with a diameter of 80 Å are completely magnetized, the equilibrium value is not yet reached for particles with a diameter of 80 to 140 Å.

At 77°K the relaxation time $\tau$, which governs the degree to which equilibrium is approximated, is appreciably higher. Now the situation around $t_3$ in Fig. 13 is present. First the magnetization increases on adsorption. At higher coverages the region of $t_2$ is entered, where the magnetization decreases, but much less than corresponds to the decrease in the equilibrium magnetization. This picture is confirmed by the measurements at different frequencies (Fig. 19). By the increase in the frequency the value of $t$ is reduced so far that the range from $t_3$ to $t_2$ is already traversed at room temperature. As is also evident from Fig. 13, the increase in magnetization is larger and the following decrease smaller at a smaller value of $t$ and, consequently, a higher frequency. This is the behavior displayed in Fig. 19; here the situation around $t_4$ in Fig. 13 is present at 77°K. In this region the slope of the magnetization-versus-time plot becomes

steeper. This causes the increase in magnetization to be larger at higher values of $t$ and, hence, at lower frequencies. Owing to the presence of the small amount of larger metal particles in the Harshaw catalyst this behavior is also maintained in the falling part of the magnetization-versus-amount-adsorbed curve.

Except in the very first stage of the process molecular oxygen oxidizes the metal particles to about 60% in one step. As a result, the magnetization of the particles is decreased so far that always a situation like that of $t_2$ in Fig. 13 is present. This implies that the magnetization is now always decreased. At low temperatures the deviation from the equilibrium magnetization is larger and, consequently, the decrease by the sorption is lower. This trend is counteracted somewhat by the use of a lower value of $M_0$ which leads to an increase in the value of $\Delta M/M_0$. This causes, at 296°K and at higher frequencies, no effect of the measuring frequency to be found beyond the measuring accuracy. At 77°K and at higher frequencies, on the other hand, the larger particles in the system do not reach their equilibrium magnetization within the measuring time after oxidation either. For these larger particles the situation around $t_4$ is present after oxidation; at lower frequencies, and hence larger values of $t$, the increase in magnetization is larger than at higher frequencies. If this increase is superposed on the dominating decrease of the smaller particles, the overall decrease in magnetization is larger at higher frequencies.

Finally, the effects of sorption from molecular oxygen and nitrous oxide on the magnetization are theoretically calculated for a rectangular particle-size distribution with $n_1 = 23\,600$ atoms ($d = 80$ Å) as the smallest, and $n_e = 31\,000$ atoms ($d = 86.5$ Å) as the largest particle. To simplify the considerations a critical particle size, $n_c$, has been assumed. Under the conditions of the measurement (temperature, field strength, and frequency) the magnetization of the larger particles is put at zero, whereas the smaller particles are supposed to reach their equilibrium magnetization. For this calculation a value of $n_c = 30\,000$ atoms ($d = 85.8$ Å) is assumed. For sorption from nitrous oxide a homogeneous distribution is assumed, whereas for sorption from molecular oxygen particle after particle is supposed to lose 18 000 atoms in one step. In Fig. 20 the results of this calculation are shown. All the essential features of, e.g., Fig. 19 are present here: a steady decrease on sorption from molecular oxygen and a passage through a maximum on adsorption from nitrous oxide. In conclusion, a difference in oxygen binding, starting from nitrous oxide or from molecular oxygen, as suggested by Selwood (*4*) is not necessary for the explanation of our results.

In the above considerations it was implicitly assumed that the value of the surface anisotropy is not influenced by the presence of nickel ions decoupled from the ferromagnetism on the surface of the metal. Although it does not necessarily follow from the experimental results presented here, much evidence from other sources points to an exchange interaction between an antiferromagnetic and an underlying ferromagnetic phase (*29*, *30*, *31*, and *16*). For this interaction Meiklejohn and Bean introduced the term *exchange anisotropy*, since in the boundary layer the magnetic coupling varies strongly from one direction to the other. In our case the moments of the ferromagnetic nickel atoms situated in the boundary layer are coupled strongly to the other metal atoms and weakly, with an exchange energy below the thermal, to the moments of the decoupled nickel ions.

As appeared from the experimental results, a thick oxide layer is formed on sorption from molecular oxygen. In this antiferromagnetic layer the direction of the magnetic moments remains fixed. Coupling of the ferromagnetic nickel atoms in the boundary layer to these stationary moments will slightly increase the anisotropy of the ferromagnetic phase. Owing to the fact, however, that the ferromagnetic core remaining after oxidation is very small, this will not affect the results.

On adsorption from nitrous oxide in the first stages of the process isolated paramagnetic nickel ions will presumably be present. Ultimately a rather thin oxide layer is formed, in which the magnetic moments

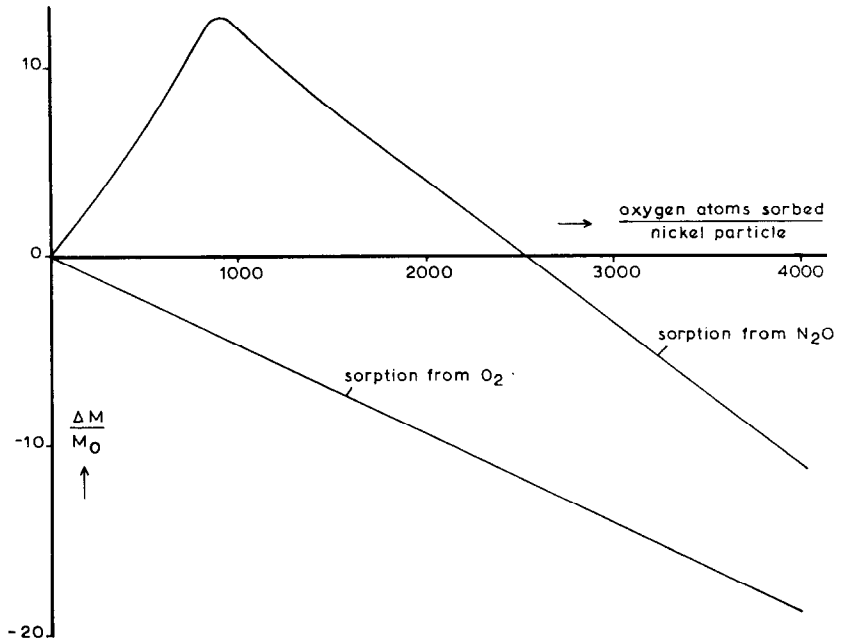


FIG. 20. Effects of sorption from nitrous oxide and from molecular oxygen on the magnetization of a hypothetic system of nickel particles as theoretically calculated. The particle-size distribution is supposed to be rectangular with $n_1$ = 23 600 atoms and $n_e$ = 31 000 atoms; the critical particle size (see text) is 30 000 atoms. In the case of sorption from molecular oxygen $n_a$ (see text) is assumed to be 30 000 atoms.

will not yet be completely fixed. Coupling to these nickel ions will decrease the anisotropy of the core per unit surface area and hence decrease $n_c$. This will intensify the trend indicated earlier, viz., an initial increase in magnetization on adsorption from nitrous oxide followed by a gradual decrease.

From the effects on both superparamagnetic and not completely superparamagnetic systems it appeared once more that explanations based on the rigid-band model are completely inadequate here, and that the influence of oxygen sorption is localized in the outer layer of the metal particle. Moreover, it was evident that the difference in effects between sorption from nitrous oxide and sorption from molecular oxygen mainly lies in the distribution of the admitted gases over the catalyst system and in the degree of oxidation of the metal particles.

## ACKNOWLEDGMENT

The authors express their gratitude to Dr. J. J. F. Scholten of this laboratory for many helpful and stimulating discussions.

## REFERENCES

1. MOORE, L. E., AND SELWOOD, P. W., *J. Am. Chem. Soc.* **78**, 697 (1956).
2. BROEDER, J. J., VAN REIJEN, L. L., AND KORSWAGEN, A. R., *J. Chim. Phys.* **54**, 37 (1957).
3. LEAK, R. J., AND SELWOOD, P. W., *J. Phys. Chem.* **64**, 1114 (1960).
4. SELWOOD, P. W., "Adsorption and Collective Paramagnetism," Chap. 10. Academic Press, New York and London, 1962.
5. GEUS, J. W., NOBEL, A. P. P., AND ZWIETERING, P., *J. Catalysis* **1**, 8 (1962).
6. HAYWARD, D. O., AND TRAPNELL, B. M. W., "Chemisorption," 2nd ed., p. 238. Butterworth, London, 1964.
7. KITTEL, C., "Introduction to Solid State Physics," 2nd ed., pp. 414, 428. Wiley, New York, 1956.
8. BECKER, R., AND DÖRING, W., "Ferromagnetismus," pp. 112–147. Springer, Berlin, 1939.
9. HEUKELOM, W., BROEDER, J. J., AND VAN REIJEN, L. L., *J. Chim. Phys.* **51**, 474 (1954).
10. BEAN, C. P., AND LIVINGSTON, J. D., *J. Appl. Phys.* **30**, Suppl., 120 S (1959).
11. ABELEDO, C., AND SELWOOD, P. W., *J. Appl. Phys.* **32**, Suppl. 229 S (1961).

*12.* NÉEL, L., *Compt. Rend* **228,** 664 (1949).
*13.* BROWN, W. F., JR., *J. Appl. Phys.* **30,** Suppl., 130 S (1959).
*14.* JACOBS, J. S., AND BEAN, C. P., *in* "Magnetism" (G. T. Rado and H. Suhl, eds.), Vol. III, p. 275. Academic Press, New York and London, 1963.
*15.* PUZEI, J. M., *Sbornik Trudov Tsentral Nauch-Issledovatel. Inst. Chernoĭ Met.* (No. 23), pp. 139–149 (1960).
*16.* BEAN, C. P., *in* "Structure and Properties of Thin Films" (C. A. Neugebauer, J. B. Newkirk, and D. A. Vermilyea, eds.), p. 347. Wiley, New York, 1959.
*17.* VAN VLECK, J. H., "The Theory of Electric and Magnetic Susceptibilities," p. 285, Oxford Univ. Press, London, 1959.
*18.* ORTON, J. W., AUZINS, P., GRIFFITHS, J. H., AND WERTZ, J. E., *Proc. Phys. Soc.* **78,** 554 (1961).
*19.* HERRING, C., *J. Appl. Phys.* **31,** Suppl., 3 S (1960).
*20.* BROOKS, H., *in* "Electronic Structure and Alloy Chemistry of Transition Elements" (P. A. Beck, ed.), p. 3. Interscience, New York, 1963.
*21.* FREEMAN, A. J., AND WATSON, R. E., *Phys. Rev.* **124,** 1439 (1961).
*22.* WATSON, R. E., AND FREEMAN, A. J., *J. Phys. Soc. Japan* **17** Suppl. B-I, 40 (1962).
*23.* ZWANZIG, R. W., *J. Chem. Phys.* **32,** 1173 (1960); GOODMAN, F. O., *J. Phys. Chem. Solids* **23,** 1269 (1962); **23,** 1491 (1962); **24,** 1451 (1963); and **26,** 85 (1965); MCCARROL, B., *J. Chem. Phys.* **39,** 1317 (1963).
*24.* DELL, R. M., KLEMPERER, D. F., AND STONE, F. S., *J. Phys. Chem.* **60,** 1586 (1956).
*25.* RUDHAM, R., AND STONE, F. S., *in* "Chemisorption" (W. A. Garner, ed.), p. 205. Butterworth, London, 1957.
*26.* KLEMPERER, D. F., AND STONE, F. S., *Proc. Roy. Soc. (London)* **A243,** 375 (1957).
*27.* LEWIS, P. H., *J. Phys. Chem.* **64,** 1103 (1960).
*28.* MACRAE, A. U., *Surface Sci.* **1,** 319 (1964).
*29.* MEIKLEJOHN, W. H., AND BEAN, C. P., *Phys. Rev.* **102,** 1413 (1956).
*30.* MEIKLEJOHN, W. H., AND BEAN, C. P., *Phys. Rev.* **105,** 904 (1957).
*31.* MEIKLEJOHN, W. H., *J. Appl. Phys.* **29,** 454 (1958).